Neurochemistry International 122 (2019) 59–72

Contents lists available at ScienceDirect

Neurochemistry International

journal homepage: www.elsevier.com/locate/neuint

Pentobarbital and other anesthetic agents induce opposite regulations of MAP kinases p-MEK and p-ERK, and upregulate p-FADD/FADD neuroplastic index in brain during hypnotic states in mice

Glòria Salort, María Álvaro-Bartolomé, Jesús A. García-Sevilla*

Laboratory of Neuropharmacology, Institut Universitari d'Investigació en Ciències de la Salut (IUNICS), University of the Balearic Islands (UIB), Institut d'investigació Sanitària Illes Balears (IdISBa), Palma de Mallorca, Spain

ARTICLE INFO

Keywords:
Pentobarbital
Isoflurane
Other anesthetic agents
MEK-ERK
p-FADD/FADD
Mouse brain

ABSTRACT

Midazolam and ketamine-induced anesthesia were recently shown to induce a disruption of MEK/ERK sequential phosphorylation with parallel upregulation of p-FADD in the mouse brain. The present study was designed to assess whether other structurally diverse anesthetic agents (pentobarbital, ethanol, chloral hydrate, isoflurane) also impair brain p-MEK to p-ERK signal and increase p-FADD during the particular time course of 'sleep' in mice. Pentobarbital (50 mg/kg)-, ethanol (4000 mg/kg)-, chloral hydrate (400 mg/kg)-, and isoflurane (2% in O_2)-induced anesthesia (range: 24–60 min) were associated with unaltered or increased p-MEK1/2 (up to +155%) and decreased p-ERK1/2 (up to −60%) contents, revealing disruption of MEK to ERK activation in mouse brain cortex. These anesthetic agents also upregulated cortical p-FADD (up to +110%), but not total FADD (moderately decreased), which resulted in increased neuroplastic/survival p-FADD/FADD ratios (up to +2.8 fold). The inhibition of pentobarbital metabolism with SKF525-A (a cytochrome P450 inhibitor) augmented barbiturate anesthesia (2.6 times) and induced a greater and sustained upregulation of p-MEK with p-ERK downregulation, as well as prolonged increases of p-FADD content and p-FADD/FADD ratio (effects lasting for more than 240 min). Pentobarbital also upregulated significantly the cortical contents of other markers of neuroplasticity such as the ERK inhibitor p-PEA-15 (up to +46%), the transcription factor NF-κB (up to +27%) and the synaptic density protein PSD-95 (up to +20%) during 'sleep'. The results reveal a paradoxical stimulation of p-MEK without the concomitant (canonical) activation of p-ERK (e.g. with pentobarbital and isoflurane), for which various molecular mechanisms are discussed. The downregulation of brain p-ERK may participate in the manifestations of adverse effects displayed by most hypnotic/anesthetic agents in clinical use (e.g. amnesia).

1. Introduction

The hypnotic/anesthetic drugs midazolam and ketamine, acting through opposing receptor systems associated with ion channels (i.e., inhibitory γ-aminobutyric acid-A ($GABA_A$) receptors and excitatory N-methyl-D-aspartate (NMDA) receptors, respectively), were recently shown to disrupt the sequential phosphorylation/activation of mitogen-activated protein (MAP) kinases p-MEK1/2 (MAP/ERK kinases; Yoon and Seger, 2006; Roskoski, 2012a) to p-ERK1/2 (Roskoski, 2012b; Buscà et al., 2016) during sleep in mouse brain cortex (Álvaro-Bartolomé et al., 2017; Salort et al., 2019). In contrast to the down-regulation of p-ERK induced by midazolam and ketamine, natural sleep promotes the upregulation of brain p-ERK1/2 (Desarnaud et al., 2011) which is followed by the induction of beneficial neuroplasticity (e.g. new synapse formation or synaptic strengthening) as observed in the visual (V1) and fronto-parietal cortices of cats (Dumoulin et al., 2015), changes that were impaired by the sedative/hypnotic drugs zolpidem and trazodone (Seibt et al., 2008; Aton et al., 2009b). Similarly, the marked reduction of p-ERK1/2 in mouse brain cortex induced by midazolam and ketamine (Álvaro-Bartolomé et al., 2017; Salort et al., 2019) was suggested to be associated with the induction of aberrant neuroplastic changes in brain circuits, which in humans could result in the expression of significant side/adverse effects (midazolam: cognitive or memory impairment, rebound insomnia upon discontinuation, rapid development of tolerance; ketamine: psychotomimetic/dissociative effects, abuse potential and neurotoxicity) that limit their routine clinical

* Corresponding author. Laboratory of Neuropharmacology (UNICS), University of the Balearic Islands (UIB), Cra. de Valldemossa km 7.5, E-07122 Palma de Mallorca, Balears, Spain.
E-mail address: jesus.garcia-sevilla@uib.es (J.A. García-Sevilla).

https://doi.org/10.1016/j.neuint.2018.11.008
Received 13 July 2018; Received in revised form 30 October 2018; Accepted 9 November 2018
Available online 10 November 2018
0197-0186/

utility.

MEK1/2 are equally competent activators of their unique substrates ERK1/2 (Pearson et al., 2001; Sweatt, 2001; Robinson et al., 2002; Roskoski, 2012a), indicating that the many functions of ERK1/2 (both enzymes displaying functional redundancy; Buscà et al., 2016) are under the control of the upstream activators MEK1/2 (Catalanotti et al., 2009; Buscà et al., 2016; it is worthy of note that Mek1 gene deletion leads to embryonic lethality in mice (Catalanotti et al., 2009). On the other hand, Fas-Associated Death Domain (FADD) is a multifunctional adaptor protein serving in the cytoplasm as an inductor of extrinsic apoptosis and as a mediator of cell survival and proliferation (Imtiyaz et al., 2009) through its p-Ser191/194 form in the nucleus (Gómez-Angelats and Cidlowski, 2003; Zhang et al., 2004; Bhojani et al., 2005; Tourneur and Chiocchia, 2010). Notably, the ratio of p-FADD to total FADD in the brain may represent a neuroplastic/survival index as reported in different experimental in vivo paradigms (reviewed in Ramos-Miguel et al., 2012). Interestingly, p-FADD and p-ERK were shown to work in concert to regulate, through the activation of transcription factors (e.g. nuclear factor-kappa B, NF-κB; Salles et al., 2014), the neurochemical events leading to sleep and neuroplasticity induced by midazolam which also involved the regulatory role of inhibitory $GABA_A$ receptors (Álvaro-Bartolomé and García-Sevilla, 2015; Álvaro-Bartolomé et al., 2017). In these complex molecular interactions leading to sleep also participate p-Ser116 PEA-15 (phosphoprotein-enriched in astrocytes of 15 kDa; see Álvaro-Bartolomé and García-Sevilla, 2015) functioning as a tight binding inhibitor of ERK activity (Formstecher et al., 2001; Callaway et al., 2007; Ramos-Miguel et al., 2010).

Against this background the present study investigated, following previous experimental designs with midazolam and ketamine (Álvaro-Bartolomé et al., 2017; Salort et al., 2019), whether other anesthetic compounds (pentobarbital, ethanol, chloral hydrate, and the inhalant agent isoflurane), but all acting through allosteric enhancements of inhibitory $GABA_A$ receptors (Mihic and Harris, 2011; Olsen, 2015), induce disruption of canonical p-MEK to p-ERK signaling and upregulation of p-FADD and p-PEA-15 in brain cortex during the various time courses of hypnosis in mice.

2. Material and methods

2.1. Hypnotic/anesthetic agents and other drugs

Pentobarbital (sodium) was a free gift from Merck-Spain (Mollet del Vallés, Barcelona). Ethanol (absolute/anhydrous > 99.5%) was purchased from Scharlau Brand-Scharlab S.L. (Sentmenat, Barcelona). Chloral hydrate (trichloroacetaldehyde hydrate) was obtained from Sigma-Aldrich (catalog C8383, batch 0073C13), Madrid, Spain. Isoflurane (FORANE^R, liquid for inhalation of the volatile anesthetic by vaporizing) was obtained from Abbot Laboratories S.A., Madrid, Spain. SKF-525A (proadifen hydrochloride) was purchased from Sigma-Aldrich (catalog P1061, batch 128K0965), and it was used as a P450 monooxygenase inhibitor to block the hepatic metabolism of pentobarbital in mice. The IUPHAR drug nomenclature for receptor allosteric ligands has been followed (Christopoulos et al., 2014): pentobarbital, ethanol, chloral hydrate and isoflurane are positive allosteric modulators (formerly called functional 'agonists') at inhibitory $GABA_A$ receptors.

2.2. Experimental animals and ethical guidelines

Swiss albino CD1 IGS male adult mice (7–9 weeks old adults; 30–40 g), originally from Charles River Laboratories (Écully, France) and then bred at the University of the Balearic Islands (UIB) animal facilities, were used. All animal care and experimental procedures were conducted according to standard ethical guidelines (ARRIVE guidelines and European Communities Council Directive 2010/63/EU) and approved by the Local Bioethical Committee of the UIB. All efforts were made to minimize the number of mice used and their suffering. The behavior experiments ('sleep test') were carried out between 08:30 a.m. and 13:00 p.m.

Table 1
'Sleep' induced by various anesthetic agents in mice: loss of righting reflex (LORR) and recovery of righting reflex (RORR).

Drug (mg/kg, i.p.) or volatile agent (% inhaled)	LORR (min)	n	RORR (min)	n
Vehicle (saline)	–	17	–	17
SKF525-A	–	6	–	6
Pentobarbital (50)	3.8 ± 0.2	28	60.0 ± 4.7	16
SKF525-A (20) + pentobarbital (50)	3.7 ± 0.2	33	157.4 ± 12.7***	14
	4.1 ± 0.5	6¶	> 250	6¶
Vehicle (saline)	–	15	–	15
Ethanol (4000)	2.3 ± 0.3	22	36.9 ± 3.5	10
Chroral hydrate (400)	4.5 ± 0.4	24	31.2 ± 5.5	11
Sham anesthesia (only O_2)	–	8	–	8
Isoflurane (2% in O_2)§	4.6 ± 0.3	17	23.8 ± 0.6	9

LORR is a marker for the hypnotic state. The time elapsing between LORR and RORR is the hypnotic effect (unconsciousness:'sleeping' time in minutes, min). SKF525-A (proadifen) is an inhibitor of pentobarbital metabolism (blockade of cytochrome P450 enzyme, CYP2 family) and it was administered 60 min before the barbiturate. ¶ This subgroup of mice (n = 6) showed a 'sleep' of very long duration (probably related to individual differences in the rate of pentobarbital metabolism) and were killed when reaching this abnormal length of time (more than 250 min) to further assess the regulation of MEK/ERK and FADD phosphorylation.
§Mice were anesthetized for 20 min in a chamber that was continuously flushed with 2% isoflurane in oxygen (O_2).
***$p < 0.001$ when compared with the saline (control) group (Mann-Whitney two-tailed *t*-test). M-W U statistics (pentobarbital *versus* SKF + pentobarbital) for LORR: 409, $p = 0.4$; for RORR: 2.00, $p < 0.0001$.

2.3. Treatments of mice with anesthetic agents and other drugs

Groups of randomly allocated mice were treated (intraperitoneal, i.p.) with selected anesthetic doses of pentobarbital (50 mg/kg, Axelrod et al., 1954), ethanol (4.0 g/kg, Sharko and Hodge, 2008) and chloral hydrate (0.4 mg/kg, Faci et al., 1998; Beland, 1999). Ethanol (anhydrous) was diluted to 20% (w/v) with saline and administered in a small volume i.p. (2 ml/kg). Deep isoflurane anesthesia in mice (2% in oxygen, Aravindan et al., 2006) was performed similarly as reported for rats by means of an induction/ventilated chamber (VIP 3000; 12 × 12 × 24 cm, serial No 0308VAP5313) (e.g. Leikas et al., 2017). Briefly, after the induction of anesthesia in mice (mean: 4.6 min; Table 1), the anesthetic concentration of isoflurane was maintained to ~2% for 20 min (O_2 flow: 0.3–0.5 L/min); control animals (sham anesthesia) were kept in the induction chamber for 20 min with flowing O_2 only. The different hypnosis times induced by these agents in mice ('sleep' of short duration lasting for 23.8–60 min; Table 1) were used as the main behavioral paradigm of the study (see below).

Other groups of mice were treated with SKF525-A alone (20 mg/kg for 1 h) or with the enzyme inhibitor (20 mg/kg) 60 min before pentobarbital (50 mg/kg) to assess the alterations of 'sleep' latency and duration of 'sleep' of the barbiturate (see Table 1). Pentobarbital is chemically stable in the brain and primarily metabolized in the liver in which the barbiturate is oxidized (Axelrod et al., 1954; Knodell et al., 1980). SKF525-A is a potent inhibitor of cytochrome P450 enzyme (CYP2 family; Zanger and Schwab, 2013) with little effect of its own, but when administered prior to a barbiturate (e.g. pentobarbital) induces a marked prolongation of the anesthetic action and inhibits its rate of biotransformation/metabolism (Axelrod et al., 1954).

In the initial group of mice (n = 39) treated with SKF525A (20 mg/

kg) and pentobarbital (50 mg/k) (n = 39), some animals (n = 6) showed a 'sleep' of very long duration and were killed around this abnormal length of time (more than 250 min; Table 1). This subgroup of 'long-sleep' mice (probably related to individual differences in the rate of pentobarbital metabolism) was used to further assess the regulation of MEK-ERK and FADD phosphorylation in parallel with a prolongation of pentobarbital-induced anesthesia.

For the different sets of experiments, 0.9% NaCl (saline 2 ml/kg, i.p.) or inhaled oxygen (in the case of sham anesthesia) was used as a vehicle control. Saline control mice killed at different time-points did not show neurochemical differences, and therefore were later pooled into one group to gain power in the statistical analyses.

2.4. 'Sleep' behaviors in mice and neurochemical analyses

The 'sleeping time' (unconsciousness) in mice induced by the chosen anesthetic agents (and doses) was monitored according to the loss of the righting reflex (LORR) and its recovery (RORR). The righting reflex (RR) being defined as the mouse ability to right itself by < 20 s when placed on its back or side on a flat surface. Drug-induced LORR in mice was the behavioral surrogate for the anesthetic action (Franks, 2008). As previously assessed for midazolam (Álvaro-Bartolomé and García-Sevilla, 2015) and ketamine (Salort et al., 2019), the time interval between drug treatment and the onset of LORR (a marker for the hypnotic state) was quantified in minutes (min) as sleep latency (see Table 1), and the duration of sleep (time to regain RORR; the hypnotic effect) lasted for 23.8–60.0 min for the various agents in mice (Table 1). LORR and RORR times were also recorded during the interaction of SKF525-A with pentobarbital, and in this experimental paradigm the hypnotic effect of the barbiturate normally lasted for 155 min (Table 1). The hypnotic doses for the different agents used in the current study did not induce mortality in mice.

At specific times after the administration of the anesthetic compounds [at LORR (0 min), during the time course of 'sleep' (between 19 and 154 min), at RORR (about 24–157 min), and after wake-up (between 83 and 200 min after RORR) (see specific time points in Figs. 2–6)], subgroups of mice were killed by decapitation without anesthesia (or immediately after isoflurane/sham anesthesia) and brain cortex (stored at −80 °C) used for neurochemical assays of the selected target proteins which were quantified by Western blot with specific antibodies (see below). The cerebral cortex was selected for examination because it is involved in the neuronal pathways of arousal and 'sleep' induced by most sedative/hypnotic drugs (see details in Álvaro-Bartolomé and García-Sevilla, 2015) and by the volatile anesthetic isoflurane (Hentschke et al., 2017), and because this brain region expresses an abundant density of inhibitory $GABA_A$ receptors (Rao et al., 2000; Schwartz and Roth, 2008; Saari et al., 2011). In previous studies with midazolam, target proteins (MEK, ERK, and FADD forms) were also quantified in brainstem and/or thalamus with similar results to those observed in mouse brain cortex (Álvaro-Bartolomé and García-Sevilla, 2015; Álvaro-Bartolomé et al., 2017). Therefore, similar changes for these molecular targets in brainstem/thalamus could also be expected after treatments with the anesthetic agents used in the present study.

2.5. Brain molecular targets, brain cortex preparation, western immunoblot, and quantification of target proteins

The basal phosphorylation state and regulation of canonical MAP kinases p-MEK1/2 and p-ERK1/2 and neuroplastic adaptor p-FADD (and p-FADD/FADD ratio) were quantified in mouse brain cortex after the acute treatments with structurally diverse hypnotic/anesthetic agents (pentobarbital, ethanol, chloral hydrate, isoflurane) and during the different time courses of anesthesia (see further details in Álvaro-Bartolomé and García-Sevilla, 2015; Álvaro-Bartolomé et al., 2017; Salort et al., 2019). During pentobarbital-induced anesthesia the status of other markers of neuroplasticity (p-PEA-15; NF-κB, and PSD-95, postsynaptic density of 95 kDa; see details in Ramos-Miguel et al., 2010, 2011; Álvaro-Bartolomé and García-Sevilla, 2015) were also quantified in mouse brain cortex.

Mouse brain cortex total homogenate with various protease and phosphatase inhibitors was prepared as previously reported (Álvaro-Bartolomé and García-Sevilla, 2015). Brain proteins (total homogenate: 40 µg protein) were resolved by electrophoresis on 10% SDS-PAGE minigels followed by immunoblotting standard procedures (García-Fuster et al., 2007, 2008). The following primary affinity-purified polyclonal antibodies (dilutions: 1:750 to 2000; overnight incubation at 4 °C) were used for western blotting: rabbit anti-p-Ser217/221 MEK1/2 (batches 31 and 49, catalog 9121, Cell Signaling, USA) or rabbit monoclonal anti-p-Ser217/221 MEK1/2 (batch 18, catalog 9154, Cell Signaling); rabbit anti-total MEK1/2 (batch 6, catalog 9122, Cell Signaling, USA); rabbit anti-p-Thr202/Tyr204 ERK1/2 (batches 26 and 27; catalog 9101, Cell Signaling, USA); mouse anti-total ERK1 (clone 631122; catalog MAB 15761, batch CEMI011, R&D Systems, USA); rabbit anti-p-Ser191 FADD (batch 1, catalog 2785, Cell Signaling, USA); rabbit anti-total FADD (batches K1407 and J1613, catalog 5559, Santa Cruz Biotechnology, USA); rabbit anti-p-Ser116 PEA-15 (batch 0100B; catalog 44-836G, Invitrogen, USA); rabbit anti-NF-κB (batch 4; catalog 8242, Cell Signaling, USA); mouse monoclonal anti-PSD-95 (clone 6G6-1C9, batch 1581097; catalog MAB1596, Millipore, USA).

The specificity of a novel rabbit monoclonal anti-p-MEK1/2 (Ser217/221) antibody (Cell Signaling, catalog 9127; see above) for phosphorylated epitopes was tested on Western blots of brain tissue, essentially as described (Ferrer-Alcón et al., 2000) (Fig. 1). Briefly,

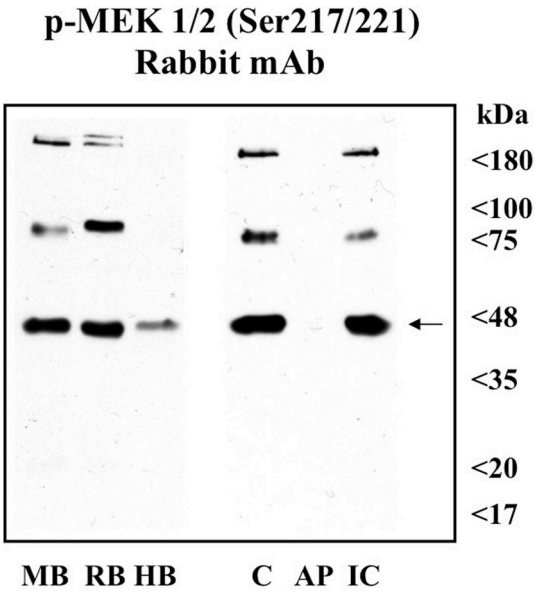

Fig. 1. Left: representative autoradiograms of Western blots depicting labelling of immunodetectable phosphorylated (p-Ser217/221) MEK1/2 forms (arrow: 45 kDa main form, and other p-forms of higher molecular masses; see Catalanotti et al., 2009) with a rabbit monoclonal antibody (Cell Signaling, catalog no. 9154) in mouse brain (MB, cerebral cortex), rat brain (RB, cerebral cortex), and human brain (HB, prefrontal cortex). Samples: 40 µg protein of total homogenate. Right: the specificity of the monoclonal antibody was assessed in dephosphorylating experiments with alkaline phosphatase (AP). Representative immunoblot for the effect of AP on p-MEK1/2 immunoreactive forms in mouse brain cortex. Total cortical homogenate was incubated at 30 °C for 15 min in the absence (C, control samples) or presence of AP (95 units). Samples containing the enzyme were also incubated with 100 mM sodium pirophosphate (IC, inhibited controls). The amount of protein loaded on the gel was 40 µg for all samples. The apparent molecular masses of p-MEK1/2 forms were determined by calibrating the blots with prestained molecular weight markers as shown on the right hand side.

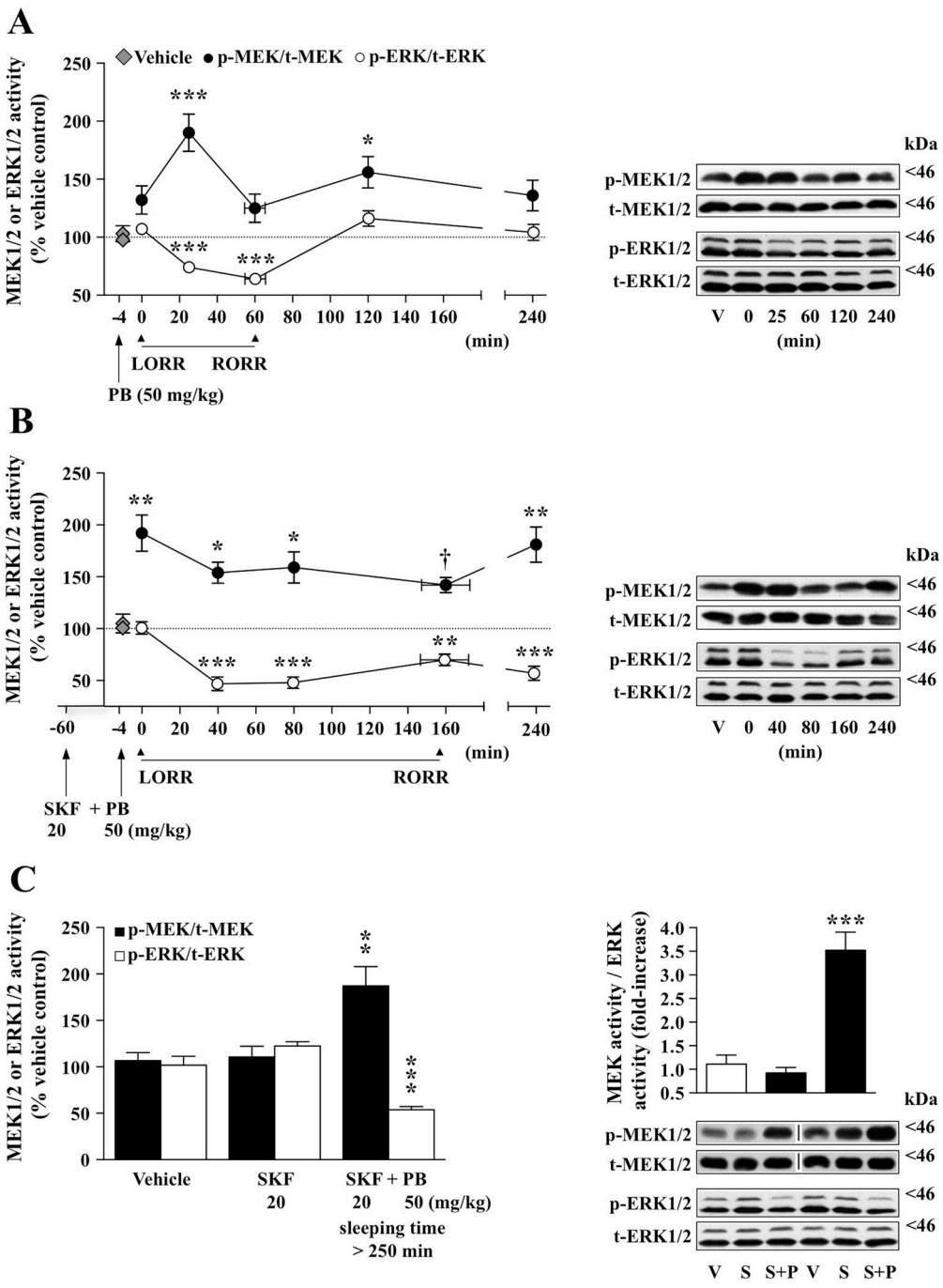

Fig. 2. (A) Regulation of cortical p-MEK1/2 (p-Ser217/221 MEK/t-MEK ratio) and p-ERK1/2 (p-Tyr204/Thr202 ERK/t-ERK ratio) enzyme activities (A, left panel) and immunocontents (A, right panel) during pentobarbital (PB, 50 mg/kg, i.p.) anesthesia (and beyond) in mice (LORR: loss of the righting reflex; RORR: recovery of the righting reflex). MEK (45 kDa) and ERK (44/42 kDa) forms were quantified at specific times after PB: at LORR (0 min, n = 6), at 25 min after LORR (n = 7), at RORR (n = 4–6), at 120 min (n = 5), and 240 min after LORR (n = 5–6). Black (MEK) and white (ERK) circles are means ± SEM (vertical bars) of n experiments per time point with an animal per experiment, and expressed as percentage of vehicle (control)-treated mice (gray diamonds, n = 9–10; the dotted line indicates the control value taken as 100%). At RORR, the horizontal bars (± SEM) denote the range of time at which mice regain the righting reflex. $^{*}p < 0.05$, $^{***}p < 0.0001$ *versus* the corresponding control (ANOVA followed by Bonferroni's test) (see Results). (A, right panel): representative immunoblots of MEK and ERK forms during and after the time course of PB-induced anesthesia in mice (V, vehicle control). (B) Effects of pretreatment with the cytochrome P450 inhibitor SKF-525A (20 mg/kg, i.p.) on the regulation of cortical p-MEK1/2 and p-ERK1 activities (left panel) and immunocontents (right panel) during PB (50 mg/kg, i.p.) sleep (and beyond) in mice: at LORR (n = 5–6), at 40 min (n = 5–6), at 80 min (n = 8–9), at RORR (n = 6), and at 240 min after LORR (n = 7–8); vehicle-control, gray diamonds, n = 5–6. Other details as above (A). $^{\dagger}p = 0.08$, $^{*}p < 0.05$, $^{**}p < 0.01$, $^{***}p < 0.001$ *versus* the corresponding control group (ANOVA followed by Bonferroni's or Sidak's test) (see Results). (B, right panel): representative immunoblots of MEK and ERK forms during and after the time course of PB + SKF-525A anesthesia in mice (V, vehicle control). (C) Regulation of cortical p-MEK/t-MEK and p-ERK/t-ERK activities (C, left panel) and MEK/ERK activity ratios (C, right panel) after SKF-525A (20 mg/kg, 60 min) and SKF + PB (50 mg/kg, > 250 min) treatments in mice. Columns are means ± SEM of n experiments (SKF, n = 5; SKF + PB, n = 6) and expressed as percentage of vehicle-treated mice (n = 5). $^{**}p < 0.01$, $^{***}p < 0.001$ *versus* the corresponding control or SKF group (ANOVA followed by Bonferroni's or Sidak's test) (see Results). (A,B,C right panels): the molecular masses of MEK and ERK forms were estimated from referenced standards.

brain cortex (mouse, rat, human) total homogenate was incubated in the absence (control, C) or presence of calf intestinal mucosa alkaline phosphatase (AP, 95 units, Product 79390, Sigma-Aldrich, Germany). Some samples containing the enzyme were also incubated with 100 mM sodium pyrophosphate (inhibited control, IC). The reaction was terminated with the addition of sodium pyrophosphate (100 mM) to control and AP samples (Ferrer-Alcón et al., 2000). This antibody characterization revealed the presence of various p-MEK1/2 forms (≈45 kDa main monomeric form, and other p-forms of higher molecular masses corresponding to homo- or hetero-dimers; see Catalanotti et al., 2009) in mouse brain (MB, cerebral cortex), rat brain (RB, cerebral cortex) and human brain (HB, prefrontal cortex) (see Fig. 1 legend). In mouse brain cortex, the content of monomeric p-MEK1/2 was similarly immunodetected with both the polyclonal (Cell Signaling, catalog 9121) and the monoclonal (Cell Signaling, catalog 9127) antibodies.

To immunodetect the total content of target kinases, independently of the protein phosphorylation state, p-kinase blots were stripped and then reprobed with the corresponding antibody for total protein, which also served as control for sample loading (see details in Álvaro-Bartolomé et al., 2017). Total FADD (~51 kDa dimeric form) and oligomeric p-Ser191 FADD (~116 kDa species; single or double band)

were immunodetected and quantified as specific FADD protein forms as previously validated in mouse, rat and human brains (García-Fuster et al., 2007, 2008; Ramos-Miguel et al., 2009). In experiments involving the quantification of FADD forms (p-FADD and total FADD) and other neuroplastic markers (p-PEA-15, NF-κB, PSD-95), the content of β-actin was also measured with a monoclonal antibody (anti-human β-actin, clone AC-15, batch 065M4837V, Sigma-Aldrich, USA; dilution 1:10,000) as a control for sample loading and protein transfer.

2.6. Quantification of target proteins

The amount of a target protein in samples of brain cortex of mice under the different treatment groups with the hypnotic agents was compared in the same gel with that of control mice (saline or sham anesthesia). The quantification procedure was assessed at least 3 times in different gels (each gel with different brain samples from control and treated mice). Percent changes in immunoreactivity with respect to

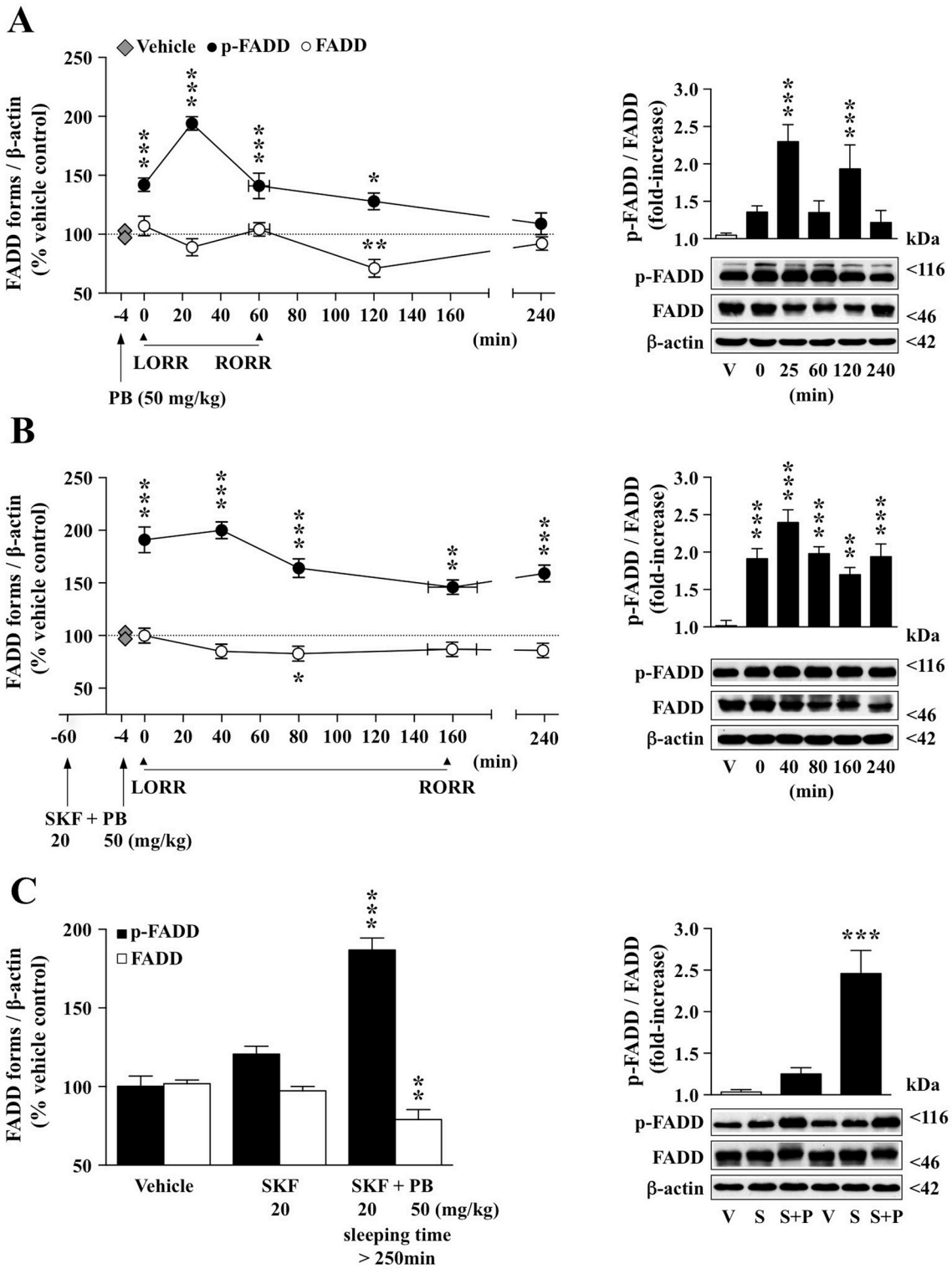

(caption on next page)

Fig. 3. (A) Regulation of cortical p-Ser191 FADD and t-FADD immunocontents (A, left panel) and p-FADD/FADD ratios (A, right panel) during pentobarbital (PB, 50 mg/kg, i.p.) anesthesia (and beyond) in mice (LORR: loss of the righting reflex; RORR: recovery of the righting reflex). p-FADD and t-FADD forms were quantified at specific times after PB: at LORR (0 min, n = 6), at 25 min after LORR (n = 7), at RORR (about 60 min, n = 6), at 120 min (n = 5), and 240 min after LORR (n = 6); vehicle (control)-treated mice (gray diamonds, n = 12). Black (p-FADD) and white (t-FADD) circles are means ± SEM (vertical bars) of n experiments; other details as for Fig. 2A. $*p < 0.05$, $**p < 0.01$, $***p < 0.001$ *versus* the corresponding control (ANOVA followed by Bonferroni's test) (see Results). (A, right panel): p-FADD/FADD ratios (black columns) and representative immunoblots (below) of p-FADD, FADD, and β-actin during and after the time course of PB-induced hypnosis in mice (V, vehicle control). (B) Effects of pretreatment with the cytochrome P450 inhibitor SKF-525A (20 mg/kg, i.p.) on the regulation of cortical p-FADD and t-FADD (left panel) and immunocontents (right panel) during PB (50 mg/kg, i.p.) anesthesia (and beyond) in mice: at LORR (n = 6), at 40 min (n = 6), at 80 min (n = 9), at RORR (n = 6), and at 240 min after LORR (n = 8); vehicle-control, gray diamonds, n = 9. Other details as for Fig. 2B. $*p < 0.05$, $**p < 0.01$, $***p < 0.001$ *versus* the corresponding control group (ANOVA followed by Bonferroni's test) (see Results). (B, right panel): p-FADD/FADD ratios (black columns) and representative immunoblots (below) of p-FADD, FADD, and β-actin during and after the time course of SKF + PB induced hypnosis in mice (V, vehicle control). (C) Regulation of cortical p-FADD and t-FADD (C, left panel) and p-FADD/t-FADD activity ratios (C, right panel) after SKF-525A (20 mg/kg, 60 min) and SKF + PB (50 mg/kg, > 250 min) treatments in mice. Columns are means ± SEM of n experiments (SKF, n = 6; SKF + PB, n = 6) and expressed as percentage of vehicle-treated mice (n = 5). $**p < 0.01$, $***p < 0.001$ *versus* the corresponding control or SKF group (ANOVA followed by Bonferroni's test (see Results). (A,B,C right panels): the molecular masses of p-FADD, FADD and β-actin were estimated from referenced standards.

control samples (100%) were calculated for each treated mouse in the various gels, and the mean value was used as a final estimate. Measurements of total/global amounts of MEK1 + MEK2 and ERK1 + ERK2 were quantified as recommended for these MAP kinases (see comments in Buscà et al., 2016). The activation of the various kinases was reported as the ratio of phosphorylated enzyme/total enzyme (p-kinase/t-kinase). Total enzyme contents in mouse brain cortex were not altered by treatments with the different hypnotic agents (see immunoblots in Figs. 2 and 4).

2.7. Processing of behavioral and neurochemical data and statistical analyses

The experimental results were expressed as mean values ± standard error of the mean (SEM). Neurochemical data conforming to the assumptions of parametric analysis were analyzed by one-way ANOVA followed by *post hoc* Bonferroni's or Sidak's multiple comparison tests or by using two-tailed Student's *t*-tests for the comparison of two groups. Behavioral data not conforming to the assumptions of parametric analysis (time for LORR and RORR of hypnotic agents) were analyzed using Mann-Whitney (M-W U statistics) two-tailed *t*-test. The assessment of correlations between parametric variables was carried out by Pearson's correlation coefficients (r) analysis. The level of significance was set at $p \leq 0.05$.

3. Results

3.1. Pentobarbital disrupts the sequential activation of p-MEK to p-ERK in mouse brain cortex during anesthesia: enhanced behavioral and neurochemical effects after pretreatment with SKF525-A, a barbiturate metabolic inhibitor

The time interval between the administration of pentobarbital (50 mg/kg, i.p.) and the onset of LORR ('sleep' latency) was about 4 min, and the duration of 'sleep' (time to regain RORR) lasted for about 60 min in mice (Table 1). During pentobarbital-induced anesthesia and beyond RORR, the cortical activation of MEK (p-MEK1/2/t-MEK1/2 ratio) was increased (ANOVA, $F[5,31] = 7.5$, $p = 0.0001$): at LORR +31 ± 12%, $p > 0.05$; at 25 min + 88 ± 16%, $p < 0.0001$; at RORR +24 ± 12%, $p > 0.05$ (Fig. 2A, left panel). This MEK upregulation (mean value from LORR to RORR: +52 ± 11%, n = 17, $t = 3.5$, $p = 0.002$) was long lasting and still sustained at 120 min (+54 ± 14%, $p < 0.02$) and 240 min (+35 ± 14%, $p > 0.05$) after LORR (Fig. 2A, left panel). In the same cortical samples, the expected parallel activation of ERK was not observed and instead a striking and opposite kinase regulation was quantified (p-ERK1/2/t-ERK1/2 ratio). Thus, ERK activity was downregulated during pentobarbital-induced anesthesia but not beyond RORR (ANOVA, $F[5,33] = 18.1$, $p < 0.0001$): at LORR +5 ± 4%, $p > 0.05$; at 25 min −27 ± 4%, $p = 0.0003$; at RORR −37 ± 3%, $p < 0.0001$). This ERK downregulation (mean value from LORR to RORR: −20 ± 5%, n = 19, $t = 2.82$, $p = 0.01$) vanished 120 min (+14 ± 7%, $p > 0.05$) and 240 min (+2 ± 7%, $p > 0.05$) after LORR (Fig. 2A, left panel). The ratio of activated p-MEK1/2 to p-ERK1/2 was markedly augmented (ANOVA, $F[5,30] = 29.4$, $p < 0.0001$) by pentobarbital (fold change compared with vehicle control, 1.0 ± 0.1): at LORR +1.2 ± 0.1, $p > 0.05$; at 25 min + 2.5 ± 0.2, $p < 0.0001$; at RORR +1.9 ± 0.1, $p < 0.0001$; but not at 120 min + 1.3 ± 0.1, $p > 0.05$; and 240 min + 1.4 ± 0.1, $p > 0.05$ after LORR. These high MEK/ERK ratios (at least during pentobarbital anesthesia) did not result in p-ERK activation (Fig. 2A, left panel).

Concerning the quantification of p-MEK (≈45 kDa monomeric form with the initial polyclonal antibody), it is of interest to note that during pentobarbital-induced anesthesia (from LORR to RORR and beyond RORR) the increased p-MEK was similarly quantified with a monoclonal antibody (see Fig. 1) in the same mouse brain cortex samples. Moreover, pentobarbital also upregulated the contents of high molecular mass p-MEK (see Fig. 1), which may correspond to p-MEK1 homodimers or p-MEK1/2 heterodimers (see Catalanotti et al., 2009) in mouse brain cortex (data not shown).

Pretreatment of mice (60 min) with the cytochrome P450 inhibitor SKF525-A (20 mg/kg, i.p.), markedly prolonged (2.6 times) pentobarbital anesthesia (RORR: 157 ± 13 min, Table 1) in parallel with sustained p-MEK1/2 upregulation (ANOVA, $F[5,30] = 4.22$, $p = 0.005$) and p-ERK1/2 downregulation (ANOVA, $F[5,34] = 17.8$, $p < 0.0001$) in brain cortex (Fig. 2B, left panel). MEK upregulation: at LORR +83 ± 18%, $p = 0.002$; at 40 min + 47 ± 10%, $p = 0.03$; at 80 min + 51 ± 15%, $p = 0.05$; at RORR (160 min) +35 ± 7%, $p = 0.08$; and at 240 min + 72 ± 17%, $p = 0.004$. ERK downregulation: at LORR −0 ± 6%, $p > 0.05$; at 40 min −53 ± 4%, $p < 0.0001$; at 80 min −52 ± 5%, $p < 0.0001$, at RORR (160 min) −31 ± 6%, $p < 0.01$, and at 240 min −44 ± 7%, $p < 0.0001$ (Fig. 2B, left panel). The observed p-MEK upregulation induced by pentobarbital after SKF525-A (mean value from LORR to RORR: +53 ± 7%, n = 24, t = 3.36, $p = 0.0023$) was very similar to that after pentobarbital alone (mean value from LORR to RORR: +52 ± 11%, n = 17, see above). In contrast, the downregulation of p-ERK after pentobarbital + SKF525-A (mean value from LORR to RORR: −36 ± 5%, n = 27, $t = 3.13$, $p = 0.004$) was significantly greater (+16%, $t = 2.36$, p = 0.023) than that induced by pentobarbital alone (mean value from LORR to RORR: −20 ± 5%, n = 19, see above).

Pretreatment with SKF525-A markedly augmented the ratio of activated p-MEK1/2 to p-ERK1/2 (ANOVA, $F[5,31] = 5.38$, $p = 0.001$) induced by pentobarbital alone (fold change compared with vehicle control, 1.0 ± 0.1): at LORR +1.9 ± 0.2, $p > 0.05$; at 40 min + 3.5 ± 0.3, $p = 0.007$; at 80 min + 3.8 ± 0.5, $p = 0.0007$; at RORR +2.1 ± 0.2, $p > 0.05$; and at 240 min + 3.0 ± 0.6, $p = 0.016$, after LORR. These high MEK/ERK ratios (at least during pentobarbital anesthesia) also predicted some activation of ERK that was not observed (Fig. 2B, left panel).

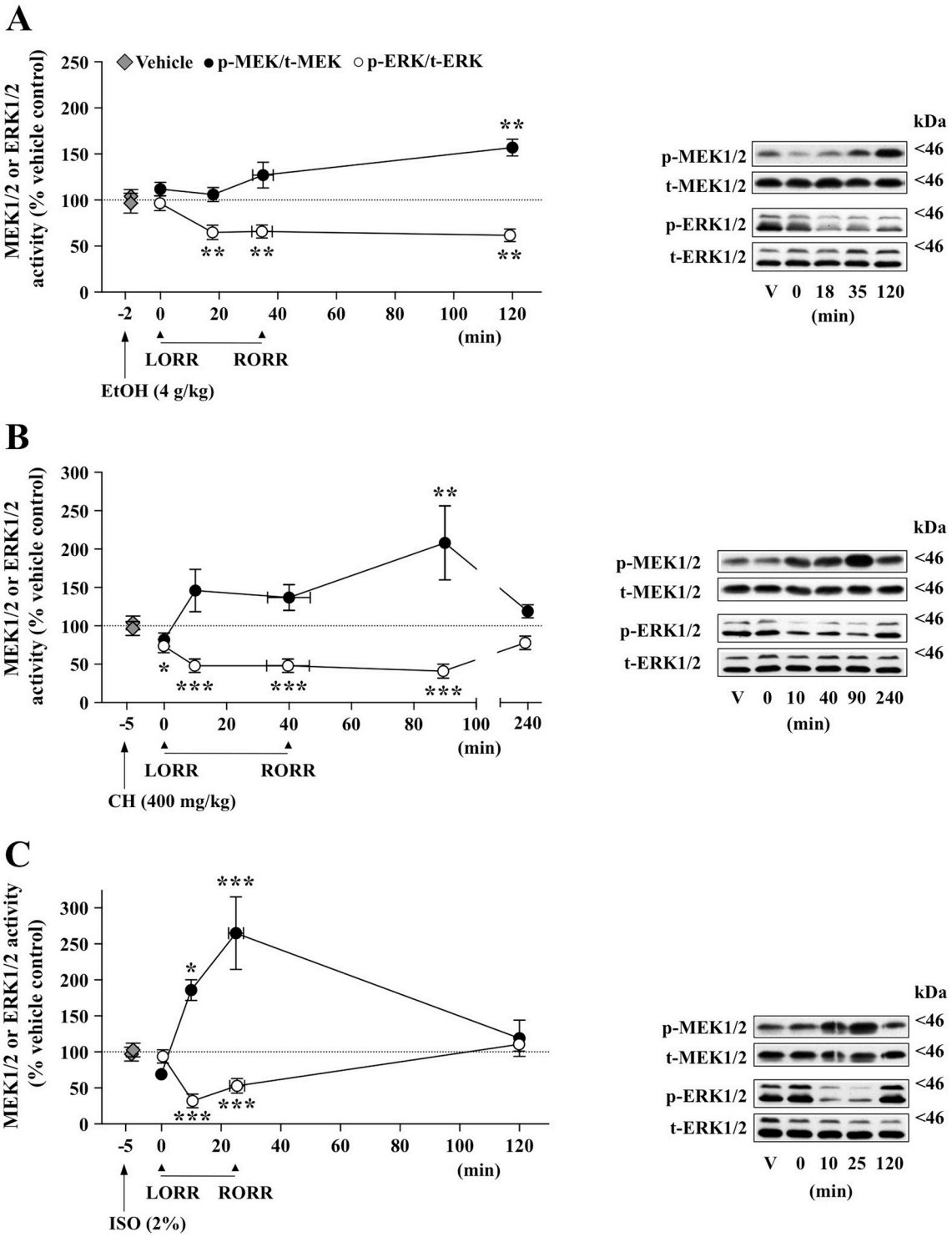

Fig. 4. Regulation of cortical p-MEK1/2 (p-Ser217/221 MEK/t-MEK ratio) and p-ERK1/2 (p-Tyr204/Thr202 ERK/t-ERK ratio) enzyme activities (left panels) and immunocontents (right panels) during (A) ethanol (EtOH, 4 g/kg, i.p.)-, (B) chloral hydrate (CH, 400 mg/kg, i.p.)-, and (C) isoflurane (ISO, 2%)-induced anesthesia (and beyond) in mice (LORR: loss of the righting reflex; RORR: recovery of the righting reflex). MEK and ERK forms were quantified at specific times after the hypnotic agent: at LORR (0 min, n = 6–8), at 10 or 18 min after LORR (n = 4–8), at RORR (about 24–40 min, n = 4–6), and at 90 or 120 min (n = 3–4), and at 240 min in the case of CH (n = 3–4) after LORR; vehicle (control)-treated mice (gray diamonds, n = 6–8). Black (MEK) and white (ERK) circles are means ± SEM (vertical bars) of n experiments; other details as for Fig. 2A. $*p < 0.05$, $**p < 0.01$, $***p < 0.001$ *versus* the corresponding control (ANOVA followed by Bonferroni's test) (see Results). (A,B,C right panels): representative immunoblots of MEK and ERK forms during and after the time courses of (A) EtOH, (B) CH, and (C) ISO-induced anesthesia in mice (V, vehicle control). (A,B,C right panels): the molecular masses of MEK and ERK forms were estimated from referenced standards.

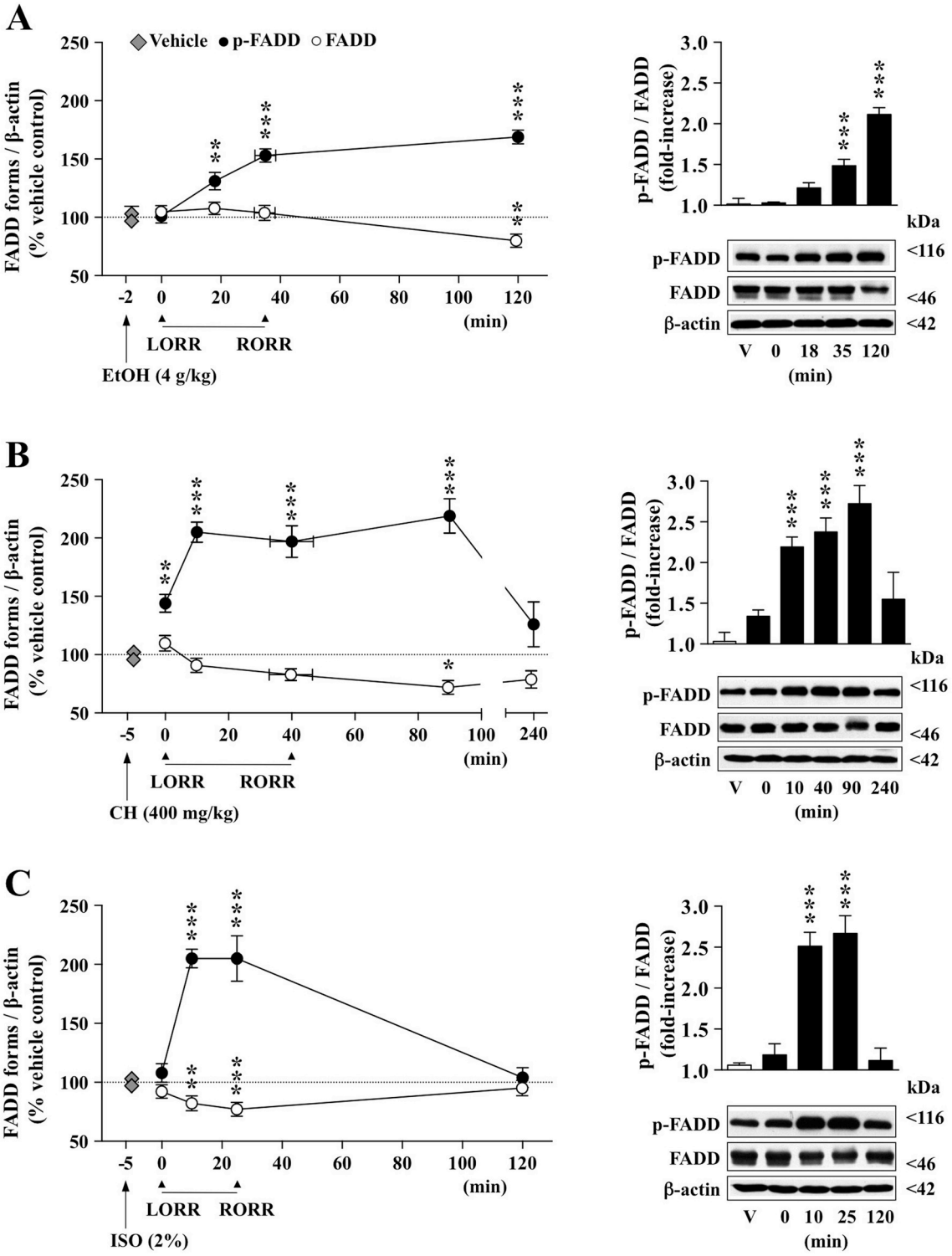

Fig. 5. Regulation of cortical p-Ser191 FADD and t-FADD immunocontents (left panels) and p-FADD/FADD ratios (right panels) during (A) ethanol (EtOH, 4 g/kg, i.p.)-, (B) chloral hydrate (CH, 400 mg/kg, i.p.)-, and (C) isoflurane (ISO, 2%)-induced anesthesia (and beyond) in mice (LORR: loss of the righting reflex; RORR: recovery of the righting reflex). p-FADD and t-FADD forms were quantified at specific times after the anesthetic agent: at LORR (0 min, n = 4–8), at 10 or 18 min after LORR (n = 4–6), at RORR (about 24–40 min, n = 5–6), and at 90 or 120 min (n = 4–5) and at 240 min in the case of CH (n = 3) after LORR; vehicle (control)-treated mice (gray diamonds, n = 7–8). Black (p-FADD) and white (t-FADD) circles are means ± SEM (vertical bars) of n experiments; other details as for Fig. 4. $*p < 0.05$, $**p < 0.01$, $***p < 0.001$ *versus* the corresponding control (ANOVA followed by Bonferroni's test) (see Results). (A,B,C right panels): p-FADD/FADD ratios (black columns) and representative immunoblots (below) of p-FADD, FADD, and β-actin during and after the time courses of (A) EtOH, (B) CH, and (C) ISO-induced anesthesia in mice (V, vehicle control). (A,B,C right panels): the molecular masses of p-FADD, FADD and β-actin were estimated from referenced standards.

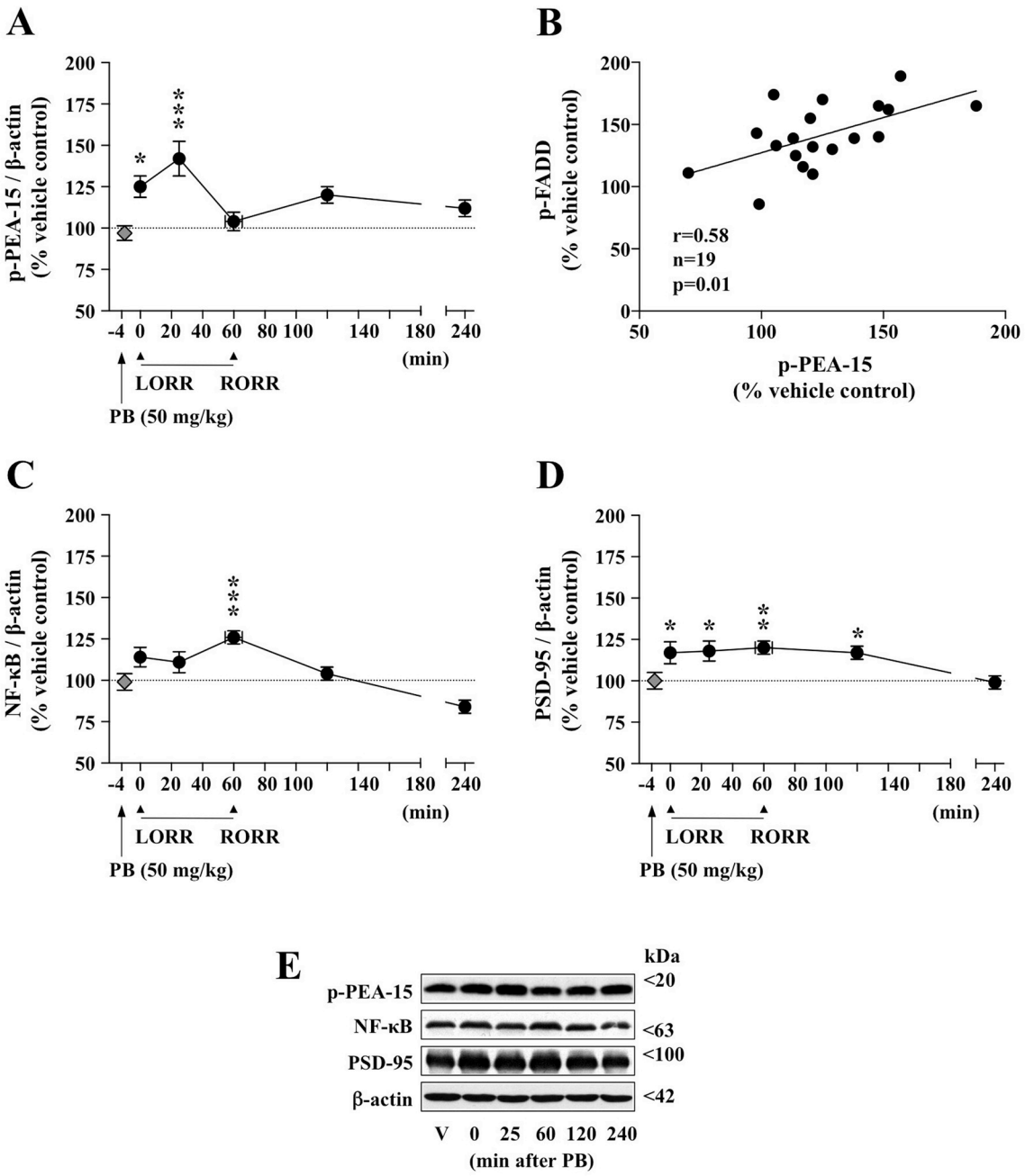

Fig. 6. (A) Regulation of cortical p-Ser116 PEA-15 immunocontent during pentobarbital (PB, 50 mg/kg, i.p.) anesthesia (and beyond) in mice (LORR: loss of the righting reflex; RORR: recovery of the righting reflex). p-PEA-15 form was quantified at specific times after PB: at LORR (0 min, n = 6), at 25 min after LORR (n = 7), at RORR (n = 6), and at 120–240 min (n = 2) after LORR; vehicle (control)-treated mice (gray diamonds, n = 11). Black (p-PEA-15) circles are means ± SEM (vertical bars) of n experiments; other details as for Fig. 2A. *$p < 0.05$, ***$p < 0.001$ *versus* control (ANOVA followed by Bonferroni's test) (see Results). (B) Scatterplot depicting a significant positive correlation between the content of p-Ser116 PEA-15 and that of p-Ser191 FADD (dependent variable) in the same brain cortex samples (A) during the time course of pentobarbital (50 mg/kg, i.p.) anesthesia in mice (from LORR to RORR). Each black circle represents a different animal. The solid line is the best fit of the correlation (r = 0.58; n = 19; $p = 0.01$). (C) Regulation of cortical NF-κB immunocontent during pentobarbital (PB, 50 mg/kg, i.p.) anesthesia (and beyond) in mice. ***$p < 0.001$ *versus* control. Other details as for (A). (D) Regulation of cortical PSD-95 immunocontent during pentobarbital (PB, 50 mg/kg, i.p.) anesthesia (and beyond) in mice. *$p < 0.05$, **$p < 0.01$ *versus* control. Other details as for (A). (E) Representative immunoblots for p-Ser116 PEA-15, NF-κB, PSD-95 and β-actin during and after the time course of pentobarbital (PB, 50 mg/kg, i.p.) anesthesia in mice.

In the initial group of mice receiving SKF525-A + pentobarbital (n = 39), some animals (n = 6) showed a very long anesthesia and were killed during the 'sleep' before reaching the state of RORR (> 250 min; see Table 1). In this subgroup of 'long-sleep' mice, cortical p-MEK1/2 was also increased (+75 ± 21%, $p = 0.006$) and p-ERK1/2 decreased (−48 ± 4%, $p < 0.0001$) compared with vehicle/control or SKF group (ANOVAs, F[2,14] = 36.5 and F[2,13] = 8.75, $p < 0.004$) (Fig. 2C, left panel), and consequently the ratio of activated p-MEK1/2 to activated p-ERK1/2 was markedly enhanced (fold-increase compared with vehicle/control, 1.1 ± 0.2): +3.2 ± 0.4, $p < 0.0001$ (Fig. 2C, right panel). Again, this high p-MEK/p-ERK ratio did not result in cortical ERK activation (Fig. 2C, left panel). SKF525-A alone (20 mg/kg, i.p., 60 min) did not significantly alter the content of p-MEK or p-ERK or p-MEK/p-ERK ratio (ratio: 0.9 ± 0.1) in mouse brain cortex (Fig. 2C, left and right panels).

3.2. Pentobarbital upregulates p-Ser191 FADD and p-FADD/FADD neuroplastic index in mouse brain cortex during anesthesia: enhanced behavioral and neurochemical effects after SKF525-A

During pentobarbital-induced anesthesia and beyond RORR, the cortical content of p-FADD was rapidly increased following the time course of the hypnosis (ANOVA, $F[5,36] = 28.8$, $p < 0.0001$): at LORR +42 ± 6%, $p < 0.0001$; at 25 min + 94 ± 5%, $p < 0.0001$; at RORR +41 ± 11%, $p < 0.0005$ (Fig. 3A, left panel). This p-FADD upregulation (mean value from LORR to RORR: 61 ± 7%, n = 19, $t = 6.32$, $p < 0.0001$) was long lasting and still sustained at 120 min (+28 ± 7%, $p = 0.02$), but not at 240 min (+9 ± 9%, $p > 0.05$), after LORR (Fig. 3A, left panel). In contrast, total cortical FADD showed a trend for a global decrease after pentobarbital treatment (ANOVA, $F[5,36] = 4.42$, $p = 0.003$): at LORR +7 ± 8%, $p > 0.05$; at 25 min −11 ± 7%, $p > 0.05$; at RORR +4 ± 4%, $p > 0.05$; at 120 min −29 ± 8%, $p = 0.004$; and at 240 min −8 ± 5%, $p > 0.05$ (Fig. 3A, left panel). Therefore, pentobarbital increased cortical p-FADD/FADD ratios (ANOVA, $F[5,36] = 10.8$, $p < 0.0001$) during anesthesia and beyond RORR (fold change compared with vehicle control, 1.0 ± 0.04): at LORR +1.4 ± 0.1, $p > 0.05$; at 25 min + 2.3 ± 0.2, $p < 0.0001$; at RORR +1.3 ± 0.2, $p > 0.05$; at 120 min (+1.9 ± 0.3, $p = 0.0006$); and at 240 min (+1.2 ± 0.2, $p > 0.05$) after LORR (Fig. 3A, right panel).

Pretreatment of mice (60 min) with the cytochrome P450 inhibitor SKF525-A (20 mg/kg, i.p.) not only prolonged the duration of anesthesia (by 2.6 times) induced by pentobarbital (RORR: 157 ± 13 min, Table 1), but it also markedly upregulated cortical p-FADD along the longer time course of hypnosis and beyond RORR (ANOVA, $F[5,38] = 21.3$, $p < 0.0001$): at LORR +91 ± 12%, $p < 0.0001$; at 40 min + 100 ± 8%, $p < 0.0001$; at 80 min + 64 ± 9%, $p < 0.0001$, at RORR (160 min) +46 ± 3%, $p = 0.001$, and at 240 min + 59 ± 8%, $p < 0.0001$ (Fig. 3B, left panel). This p-FADD upregulation (mean value from LORR to RORR: 74 ± 6%, n = 27, t = 7.10, $p < 0.0001$) (Fig. 3B, left panel) was only slightly higher (+13%, t = 1.50, $p > 0.05$) than that induced by pentobarbital alone (61 ± 7%, n = 19) (Fig. 3A, left panel). In contrast to p-FADD, total FADD content was marginally reduced (ANOVA, $F[5,38] = 3.52$, $p = 0.01$), except at 80 min (−16 ± 2%, $p = 0.02$) after LORR in mouse brain cortex (Fig. 3B, left panel). Therefore, the inhibition of pentobarbital metabolism (with SKF525-A) markedly increased (ANOVA, $F[5,38] = 14.6$, $p < 0.0001$) cortical p-FADD/FADD ratios (fold change compared with vehicle control, 1.0 ± 0.07): at LORR +1.9 ± 0.1, $p < 0.0001$; at 40 min + 2.4 ± 0.2, $p < 0.0001$; at 80 min + 2.0 ± 0.1, $p < 0.0001$, at RORR (160 min) +1.7 ± 0.1, $p = 0.002$; and at 240 min + 1.9 ± 0.2, $p < 0.0001$, after LORR (Fig. 3B, right panel). These p-FADD/FADD ratios for SKF525-A + pentobarbital (2.0 ± 0.1%, n = 27) were nonsignificantly higher (+30%, $t = 1.97$, $p = 0.055$) than those induced by pentobarbital alone (1.7 ± 0.1%, n = 19) (compared ratios in Fig. 3A/B, right panels).

In the initial group of mice receiving SKF525-A + pentobarbital (n = 39), some animals (n = 6) showed a very long anesthesia and were killed during the 'sleep' before reaching the state of RORR (see Table 1). In this subgroup of 'long-sleep' mice, cortical p-FADD was also increased (+87 ± 8%, $p < 0.0001$) and total FADD decreased (−23 ± 6%, $p = 0.006$) compared with vehicle/control or SKF group (ANOVA, $F[2,14] = 49.0$ and 7.5; at least $p < 0.005$) (Fig. 3C, left panel). In this particular pentobarbital experiment, cortical p-FADD/FADD ratio (compared with vehicle control, 1.0 ± 0.05) was also increased: 2.5 ± 0.3, n = 6) (Fig. 3C, right panel). SKF525-A alone (20 mg/kg, i.p., 60 min) did not significantly alter the content of p-FADD or total FADD or FADD/FADD ratio (ratio: +1.2 ± 0.08) in mouse brain cortex (Fig. 3C, left and right panels).

3.3. Ethanol, chloral hydrate and isoflurane disrupt the sequential activation of p-MEK to p-ERK, and upregulate p-Ser191 FADD and p-FADD/FADD neuroplastic index in mouse brain cortex during anesthesia

Similarly to pentobarbital, other structurally diverse anesthetic agents also altered MEK-ERK sequential signaling and enhanced the content of survival p-FADD (and p-FADD/FADD ratio) in mouse brain. The time interval between the administrations of ethanol (4 g/kg, i.p), chloral hydrate (0.4 g/kg, i.p) or isoflurane (2% inhaled in O_2) and the onset of LORR ('sleep' latency) varied from 2.3 to 4.6 min, and the duration of 'sleep' (time to regain RORR) lasted for 23.8–36.9 min in mice (Table 1).

During ethanol-induced anesthesia, MEK activity (p-MEK1/2/t-MEK1/2 ratio) was not altered in mouse brain cortex (from LORR to RORR), but it was increased 120 min after LORR (+51 ± 9%, p = 0.005) (Fig. 4A). In the same cortical samples, ERK activity (p-ERK1/2/t-ERK1/2 ratio) was downregulated during ethanol-induced anesthesia and beyond RORR (ANOVA, $F[4,24] = 6.77$, $p = 0.0008$): at LORR −6 ± 8%, $p > 0.05$; at 18 min −37 ± 5%, $p = 0.005$; at RORR −36 ± 4%, $p = 0.006$; at 120 min after LORR −40 ± 5%, $p = 0.007$ (Fig. 4A). On the other hand, ethanol increased cortical p-FADD content during anesthesia and beyond RORR (ANOVA, $F[4,24] = 22.2$, $p < 0.0001$): at LORR +1 ± 4%, $p > 0.05$; at 18 min + 30 ± 8%, $p = 0.005$; at RORR +51 ± 6%, $p < 0.0001$; and at 120 min + 67 ± 6%, $p < 0.0001$, after LORR (Fig. 5A). In contrast, total FADD was not altered in mouse brain cortex (from LORR to RORR), but it was decreased 120 min after LORR (−21 ± 1%, $p = 0.01$) (Fig. 5A). Consequently, ethanol increased cortical p-FADD/FADD ratios (ANOVA, $F[4,24] = 39.4$, $p < 0.0001$) during 'sleep' and beyond RORR (fold change compared with vehicle control; range: +1.21 to +2.12, $p < 0.01$) (Fig. 5A, right panel).

During chloral hydrate-induced anesthesia, MEK activity was not altered in mouse brain cortex (from LORR to RORR), but it was significantly increased 90 min after LORR (+108 ± 49%, $p = 0.002$) (Fig. 4B). In the same cortical samples, ERK activity was downregulated during chloral hydrate-induced 'sleep' (from LORR to RORR) and beyond RORR (ANOVA, $F[5,25] = 10.2$, $p < 0.0001$): at LORR −27 ± 9%, $p = 0.02$; at 10 min −52 ± 7%, $p = 0.0003$; at RORR −52 ± 5%, $p < 0.0001$; and at 90 min −59 ± 7%, $p < 0.0001$, and 240 min −23 ± 5%, $p > 0.05$, after LORR (Fig. 4B). Notably, chloral hydrate markedly increased cortical p-FADD content from LORR to RORR and beyond RORR (ANOVA, $F[5,28] = 23.3$, $p < 0.0001$): at LORR +48 ± 8%, $p = 0.003$; at 10 min + 111 ± 9%, $p < 0.0001$; at RORR +103 ± 14%, $p < 0.0001$; and at 90 min + 126 ± 15%, $p < 0.0001$, and 240 min + 30 ± 19%, $p > 0.05$, after LORR (Fig. 5B). In contrast, total FADD was not altered in mouse brain cortex (from LORR to RORR) but it was decreased 90 min after LORR (−25 ± 6%, $p = 0.01$) (Fig. 5B). Thus, chloral hydrate increased cortical p-FADD/FADD ratios (ANOVA, $F[5,26] = 22.2$, $p < 0.0001$) during 'sleep' and beyond RORR (fold change compared with vehicle control; range: +1.34 to +2.72, $p < 0.01$) (Fig. 5B, right panel).

Deep but brief isoflurane anesthesia rapidly increased MEK activity from LORR to RORR, but not beyond RORR, in mouse brain cortex (ANOVA, $F[4,18] = 10.9$, $p = 0.0001$): at LORR −30 ± 2%, $p > 0.05$; at 10 min + 90 ± 14%, $p < 0.05$; at RORR +170 ± 50%, $p = 0.0002$; and at 120 min + 21 ± 25%, $p > 0.05$, after LORR (Fig. 4C). In the same cortical samples, isoflurane downregulated ERK activity from LORR to RORR, but not beyond RORR (ANOVA, $F[4,20] = 22.4$, $p < 0.0001$): at LORR −7 ± 10%, $p > 0.05$; at 10 min −68 ± 7%, $p < 0.0001$; at RORR −48 ± 10%, $p < 0.0001$; and at 120 min + 10 ± 5%, $p > 0.05$, after LORR (Fig. 4C). Notably, isoflurane markedly increased cortical p-FADD (ANOVA, $F[4,20] = 28.9$, $p < 0.0001$): at LORR +9 ± 8%, $p > 0.05$; at 10 min + 107 ± 8%, $p < 0.0001$; at RORR +107 ± 19%, $p < 0.0001$; and decreased total FADD (ANOVA, $F[4,20] = 8.37$, $p = 0.0004$: at LORR −8 ± 4%, $p > 0.05$; at 10 min −18 ± 4%,

$p = 0.006$; at RORR −23 ± 3%, $p = 0.0002$) contents from LORR to RORR, but not beyond RORR, in mouse brain cortex (Fig. 5C). Consequently, isoflurane increased cortical p-FADD/FADD ratios (ANOVA, $F[4,20] = 36.6$, $p < 0.0001$) during anesthesia and beyond RORR (fold change compared with vehicle control; range: +1.19 to +2.66, $p < 0.01$) (Fig. 5C, right panel).

3.4. Pentobarbital-induced anesthesia is associated with upregulation of classic markers of neuroplasticity in mouse brain cortex

Pentobarbital, as the prototypical and more versatile drug of the present group of anesthetic agents, was further investigated to assess the possible modulation of relevant markers of neuroplasticity (other than p-Ser191 FADD) in mouse brain cortex.

During pentobarbital (50 mg/kg, i.p.)-induced anesthesia, the cortical content of p-Ser116 PEA-15, a cytoplasmic partner in p-Ser191 FADD signaling, was increased from LORR to RORR (ANOVA, $F[3,26] = 8.62$, $p = 0.0004$): at LORR +29 ± 7%, $p = 0.03$, n = 6; at 25 min + 46 ± 11%, $p = 0.0002$, n = 7; at RORR +7 ± 6%, $p > 0.05$, n = 6; vehicle/control, n = 11 (Fig. 6A). Remarkably, the upregulation of cortical p-PEA-15 content during anesthesia correlated positively with that of p-FADD (dependent variable) in the same mouse brain samples ($r = 0.58$, n = 19, $p = 0.01$) (Fig. 6B).

The anesthetic action of pentobarbital (50 mg/kg) also increased the content of NF-κB, a pleotropic transcription factor associated with p-FADD and p-PEA-15, from LORR to RORR in mouse brain cortex (ANOVA, $F[5,32] = 10.2$, $p < 0.0001$): at LORR +15 ± 6%, $p > 0.05$, n = 6; at 25 min + 12 ± 6%, $p > 0.05$, n = 7; at RORR +27 ± 2%, $p = 0.0005$, n = 5; vehicle/control, 99 ± 3%, n = 9 (Fig. 6C).

Pentobarbital (50 mg/kg)-induced anesthesia also upregulated PSD-95, a postsynaptic protein marker of synaptic density, from LORR to RORR and even beyond RORR in mouse brain cortex (ANOVA, $F[5,33] = 5.25$, $p = 0.0012$): at LORR +17 ± 7%, p = 0.04, n = 6; at 25 min + 18 ± 6%, $p = 0.02$, n = 7; at RORR +20 ± 2%, $p = 0.008$, n = 6; at 120 min + 17 ± 3%, $p < 0.05$, n = 5; and at 240 min −1 ± 3%, $p > 0.05$, n = 6; vehicle/control, n = 9 (Fig. 6D).

4. Discussion

The purpose of this behavior/neurochemical study was to investigate if similarly to the benzodiazepine midazolam (Álvaro-Bartolomé et al., 2017) and the dissociative anesthetic ketamine (Salort et al., 2019), other structurally diverse anesthetic agents deregulate the concomitant phosphorylation of MAP kinases MEK to ERK, and induce in parallel the upregulation of multifunctional FADD protein in mouse brain cortex during the states of unconsciousness. The major findings reveal that (1) the sequential phosphorylation/activation of cortical MEK (p-MEK1/2/t-ERK1/2 ratio) to p-ERK (p-ERK1/2/t-ERK1/2 ratio), both involved in memory and synaptic plasticity, is disrupted during the time courses of anesthesia ('sleep' from LORR to RORR, and even beyond RORR) induced by pentobarbital, ethanol, chloral hydrate and isoflurane (i.e. increased or unaltered MEK activity with ERK downregulation), and (2) these anesthetic agents also promoted the upregulation of anti-apoptotic/survival p-FADD and increased neuroplastic p-FADD/FADD ratio in mouse brain cortex.

Notably, the inhibition of pentobarbital metabolism with SKF525-A (a cytochrome P450 inhibitor; Axelrod et al., 1954; Knodell et al., 1980) in mice not only augmented barbiturate anesthesia but also induced a sustained upregulation of MEK activity and ERK downregulation (Fig. 2B), with prolonged increases of p-FADD content and p-FADD/FADD ratio (Fig. 3B) in brain cortex. Also notable was the marked and sustained upregulation of cortical p-FADD and p-FADD/FADD ratio induced by chloral hydrate (Fig. 5B), which most probably was due to the additive effect of its main active metabolite trichloroethanol, whose elimination half-life is of several hours (Faci et al., 1998; Shroads et al., 2015). The enhancing effects of SKF525-A on pentobarbital anesthesia and brain MEK/ERK and p-FADD/FADD regulations, as well as the marked effect of chloral hydrate/trichloroethanol upregulating cortical p-FADD content, further demonstrated the relevant role of these proteins in anesthetic states induced by different agents.

Remarkably, the common regulation and in the same direction of p-MEK/p-ERK activities and p-FADD/FADD ratio by different anesthetic agents such as pentobarbital, ethanol, chloral hydrate and isoflurane, and also by anesthetic doses of midazolam (Álvaro-Bartolomé and García-Sevilla, 2015; Álvaro-Bartolomé et al., 2017) and anesthetic/subanesthetic doses of ketamine (Salort et al., 2019), clearly indicate that these molecular targets participate in the complex neurochemical events leading to drug-induced sedation/'sleep'/deep anesthesia, and probably also to the development of aberrant neuroplastic changes associated with the downregulation of p-ERK in the brain, which could underlie some adverse effects of hypnotic drugs in their clinical uses (Álvaro-Bartolomé et al., 2017; Mihic and Harris, 2011; see further discussion below). In marked contrast, natural sleep was shown to promote upregulation of ERK activity (leading to sleep maintenance via suppression of wakefulness) in the rat brainstem (Desarnaud et al., 2011) and in the cat cerebral cortex (Aton et al., 2009a; Dumoulin et al., 2015), with the induction of beneficial plasticity as observed in the primary visual cortex of cats (Dumoulin et al., 2015). Moreover and in line with the current findings, the hypnotic drugs zolpidem (Seibt et al., 2008) and trazodone (Aton et al., 2009b) were shown to reduce or impair cortical neuroplasticity induced by natural sleep (Dumoulin et al., 2015).

Notably, the anesthetic actions of pentobarbital (including its interaction with SKF-525A), ethanol, chloral hydrate (and its metabolite trichloroethanol), and isoflurane were associated with upregulation of p-FADD content (and p-FADD/FADD ratio), and in the case of pentobarbital-induced anesthesia also with increased contents of p-PEA-15 (a partner of FADD and a negative regulator of ERK; see below), NF-κB (a pleotropic transcription factor, Salles et al., 2014) and PSD-95 (a marker of synaptic density; Yang et al., 2014; Coley and Gao, 2018) in mouse brain cortex. These results clearly indicated the involvement of FADD and associated partners in anesthesia (e.g. pentobarbital)-induced neuroplasticity, as previously shown for midazolam (Álvaro-Bartolomé and García-Sevilla, 2015) and ketamine (Salort et al., 2019). These findings are also in line with previous studies that demonstrated the participation of FADD and p-FADD forms (and p-FADD/FADD ratio as a neuroplastic/survival index) in the behavioral/neurochemical actions of different drugs in various vivo experimental paradigms in the rodent and human brains (García-Fuster et al., 2008; Ramos-Miguel et al., 2009, 2010; 2012; Álvaro-Bartolomé et al., 2011).

It is well known that the effects of most sedative/hypnotic/anesthetic agents (Mihic and Harris, 2011; Saari et al., 2011) are mediated through allosteric activations of $GABA_A$ receptors (Christopoulos et al., 2014; Olsen, 2015) leading to potentiation of GABAergic neurotransmission (Campagna et al., 2003; Franks, 2008; Alkire et al., 2008; D'Hulst et al., 2009). Thus, numerous studies have documented the direct or indirect involvement of specific $GABA_A$ receptor subtypes (sensitive to the orthosteric competitive antagonist bicuculline or to the allosteric negative modulator flumazenil) mediating the various effects of pentobarbital (Steinbach and Akk, 2001; Zeller et al., 2007; Jeon et al., 2015), ethanol (Suzdak et al., 1986; Kumar et al., 2009), chloral hydrate/trichloroethanol (Garrett and Gan, 1998; Beland, 1999), and isoflurane (Harrison et al., 1993; Vahle-Hinz et al., 2001; Jia et al., 2008). Therefore, GABAergic mechanisms associated with the MEK-ERK disruption induced by the benzodiazepine midazolam (see Álvaro-Bartolomé et al., 2017), as well as other molecular mechanisms (i.e. PEA-15 as a potent ERK inhibitor; see below), could be postulated for the anesthetic agents used in the present investigation.

In previous studies, acute treatment with ethanol in C57BL/6CR mice (Kalluri and Ticku, 2002) and isoflurane in Sprague-Dawley rats (Takamura et al., 2008) were reported to downregulate the brain

content of p-ERK, and in vitro exposure to pentobarbital reduced p-ERK in rat C6 glioma cells (Xie et al., 2009), but these works did not assess the activity of the upstream kinase p-MEK, and therefore the possible deregulation from p-MEK to p-ERK could not be observed. Indeed, the most interesting aspect of the current study is the discrepancy between the regulation of p-MEK (kinase activity markedly increased or unaltered) and that of p-ERK (kinase activity decreased) induced by different anesthetic agents (pentobarbital, ethanol, choral hydrate and isoflurane) in mouse brain cortex. In fact, a significant negative relationship was observed when individual p-MEK and p-ERK data (in the same mice cortical samples) for the investigated anesthetic agents were combined and analyzed together ($r = -0.22$; $n = 76$; $p = 0.026$) (Fig. 7). These were striking findings when a large increase in MEK activation in brain would be expected to translate into substantial activation of its exclusive substrate ERK (see Introduction). Furthermore, ERK kinases are very stable proteins with a long half-life for both ERK1 ($t_{1/2} = 68$ h) and ERK2 ($t_{1/2} = 53$ h) (reviewed in Buscà et al., 2016); this great ERK stability discounted the involvement of some enzyme degradation in the downregulation of ERK activity (quantified as p-ERK1/2/t-ERK1/2 ratio) induced by anesthetic agents.

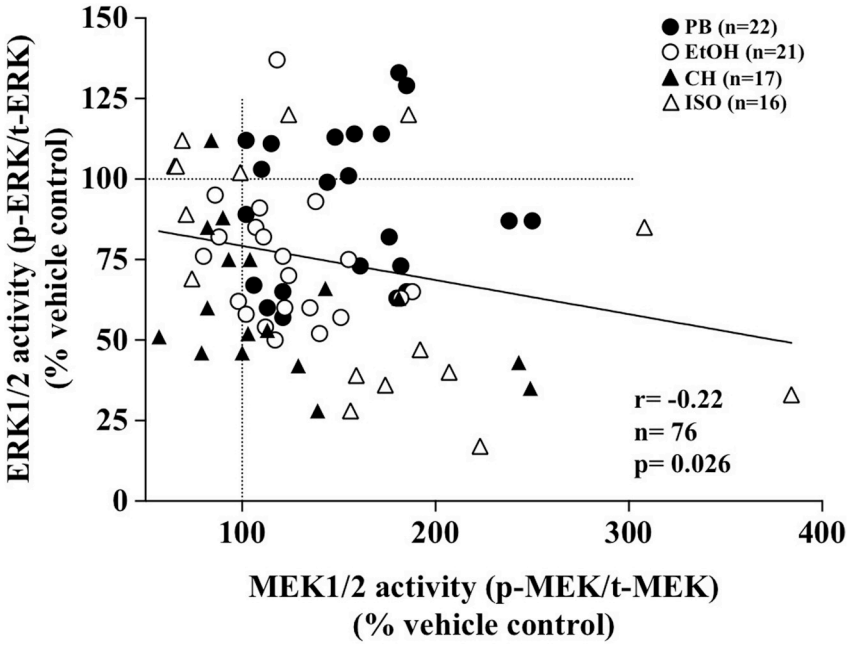

Fig. 7. Scatterplot depicting a significant inverse correlation between MEK1/2 and ERK1/2 (dependent variable) MAP kinase activities in brain cortex during the anesthetic effects induced by pentobarbital (PB, 50 mg/kg, i.p.), ethanol (EtOH, 4 g/kg, i.p.), chloral hydrate (CH, 400 mg/kg, i.p.) and isoflurane (ISO, 2%) in mice (from LORR to 90 or 120 min). Each symbol represents a different animal. The dotted lines indicate the control values (% vehicle) for MEK and ERK (taken as 100%). The solid line is the best fit of the correlation ($r = -0.22$; $n = 76$; $p = 0.026$).

The paradoxical marked stimulation of MEK without the concomitant activation of ERK in mouse brain cortex (present study; Álvaro-Bartolomé et al., 2017; Salort et al., 2019) had been observed previously in various rat brain regions (including the cerebral cortex) under different experimental paradigms, such as acute swim stress (Shen et al., 2004) and treatment with the μ-opioid receptor agonist fentanyl (low dose: 0.1 mg/kg, i.p., Ramos-Miguel and García-Sevilla, 2012), but the underlying mechanisms remained obscure (see early proposed explanations in Shen et al., 2004). More recently, various molecular mechanisms have been disclosed which can explain the disruption of brain MEK-ERK sequential activities (i.e. roles of inactivated p-Thr286 MEK1 and/or phosphatase MPK-3, both upregulated) induced by unrelated drugs such as fentanyl (Ramos-Miguel and García-Sevilla, 2012) and midazolam (Álvaro-Bartolomé et al., 2017). In the current study, however, pentobarbital (50 mg/kg, i.p.)-induced anesthesia (RORR at 60 min, and post RORR up to 240 min) did not alter the contents of p-Thr286 MEK1 and MPK-1,2,3 in mouse brain cortex (data not shown), indicating that other molecular mechanisms must be responsible for the observed p-ERK downregulation (see below, PEA-15 as a potent inhibitor of ERK).

It is known that one rapid action of anesthetic agents is to induce hypothermia (< 36 °C) in experimental animals and humans during surgical anesthesia, mainly due to hemodynamic (vasodilation) effects (Patel et al., 2011). Recently, the inhibition of brain p-ERK1/2 (the status of p-MEK was not assessed) by isoflurane (inhalant anesthetic) and propofol (intravenous sedative/anesthetic) was suggested to be related to the hypothermia (rectal temperature) induced by these agents in Fisher 344 rats and C57BL/6J mice (Whittington et al., 2013); under normothermic conditions (experiments performed in a warmed Plexiglas anesthesia chamber), isoflurane did not decrease normal body temperature (37 °C) or the brain content of p-ERK1/2 in Fisher 344 rats (Whittington et al., 2013). In other studies, however, activation of cannabinoid CB_1 receptor with the selective agonist WIN55212-2 induced marked hypothermia with the concomitant parallel upregulation of brain p-MEK (63%) and p-ERK1/2 (24%/28%) in Sprague-Dawley rats (Moranta et al., 2007). Therefore, the hypothermic response induced by different classes of drugs (inducing or not anesthesia) not always results in downregulation of p-ERK1/2 in the brain of rodents.

In addition, other mechanisms can be postulated to explain the disruption of p-MEK (increase) to p-ERK (decrease) signal induced by pentobarbital. The current results demonstrate that pentobarbital-induced hypnosis also increased p-PEA-15 content, which in turn showed a positive correlation with that of p-FADD (dependent variable) in the same mouse cortical samples (Fig. 6A/B); both molecules involved in neuroplasticity (see above). On the other hand, the scaffolding protein PEA-15 was reported to inhibit ERK activity (and its nuclear transport), and therefore classic p-ERK1/2 downstream targets can be downregulated (Formstecher et al., 2001; Chou et al., 2003; Callaway et al., 2007). In fact, various structures of PEA-15 were shown to bind to different p-states of ERK (PEA-ERK complex) providing a mechanism for disrupting key features of active ERK2 (Mace et al., 2013); thus, PEA-15 overexpression in culture markedly reduced ERK-dependent gene transcription (Krueger et al., 2005). In this context, it is worth nothing that pentobarbital-induced anesthesia was associated with increased p-PEA-15 (Fig. 6) and decreased p-ERK activity (Fig. 2A/B), and that there was a trend for an inverse correlation between the contents of these two proteins (p-ERK as the dependent variable) in the same mouse cortical samples ($r = -0.19$, $n = 56$, $p = 0.077$). Altogether,

these findings suggest that ERK downregulation is linked to the upregulation of PEA-15 (ERK1/2 inhibitor) in mouse brain. This latter molecular mechanism could also explain in part the downregulation of cortical p-ERK induced by ethanol, chloral hydrate and isoflurane in mice.

5. Conclusion

The sequential activation of cortical MEK (p-MEK1/2/t-MEK1/2 ratio) to p-ERK (p-ERK1/2/t-ERK1/2 ratio), both kinases involved in memory and synaptic plasticity, was disrupted (i.e. increased or unaltered MEK activity with downregulation of ERK activity) during the time courses of anesthesia induced by pentobarbital, ethanol, chloral hydrate and isoflurane in mice. Furthermore, these anesthetic agents also promoted the upregulation of p-FADD (an anti-apoptotic/survival protein) and increased p-FADD/FADD ratio (a neuroplastic index) and p-PEA-15 (an ERK inhibitor) content for pentobarbital in mouse brain cortex. The abnormal downregulation of p-ERK in brain may participate in the manifestations of adverse effects displayed by most hypnotic/anesthetic drugs in clinical use (e.g. amnesia, rebound insomnia, development of drug tolerance).

Disclosure

The authors declare no conflict of interest.

Funding and acknowledgements

The study was partly supported by grants SAF2011-29918 and SAF2014-55903-R from Ministerio de Economía y Competitividad (MINECO) and Fondo Europeo de Desarrollo Regional (FEDER), Spain. Jesús A. García-Sevilla is Professor Emeritus of Pharmacology at Universitat de les Illes Balears (UIB), Palma de Mallorca, and Member Emeritus of the Institut d'Estudis Catalans (IEC), Barcelona, Spain.

References

Alkire, M.T., Hudetz, A.G., Tononi, G., 2008. Consciousness and anesthesia. Science 322, 876–880.

Álvaro-Bartolomé, M., La Harpe, R., Callado, L.F., Meana, J.J., García-Sevilla, J.A., 2011. Molecular adaptations of apoptotic pathways and signaling partners in the cerebral cortex of human cocaine addicts and cocaine-treated rats. Neuroscience 196, 1–15.

Álvaro-Bartolomé, M., García-Sevilla, J.A., 2015. The neuroplastic index p-FADD/FADD and phosphoprotein PEA-15, interacting at $GABA_A$ receptor, are upregulated in brain cortex during midazolam-induced hypnosis in mice. Eur. Neuropsychopharmacol 25, 2131–2144.

Álvaro-Bartolomé, M., Salort, G., García-Sevilla, J.A., 2017. Disruption of brain MEK-ERK sequential phosphorylation and activation during midazolam-induced hypnosis in mice: roles of $GABA_A$ receptor, MEK1 inactivation, and phosphatase MKP-3. Prog. Neuro-Psychopharmacol. Biol. Psychiatry 75, 84–93.

Aravindan, N., Cata, J.P., Hoffman, L., Dougherty, P.M., Riedel, B.J., Price, K.J., Shaw, A.D., 2006. Effects of isoflurane, pentobarbital, and urethane on apoptosis and apoptotic signal transduction in rat kidney. Acta Anaesthesiol. Scand. 50, 1229–1237.

Aton, S.J., Seibt, J., Dumoulin, M., Jha, S.K., Steinmetz, N., Coleman, T., Naidoo, N., Frank, M.G., 2009a. Mechanisms of sleep-dependent consolidation of cortical plasticity. Neuron 61, 454–466.

Aton, S.J., Seibt, J., Dumoulin, M.C., Coleman, T., Shiraishi, M., Frank, M.G., 2009b. The sedating antidepressant trazodone impairs sleep-dependent cortical plasticity. PloS One 4 (7). https://doi.org/10.1371/journal.pone.0006078. e6078.

Axelrod, J., Reichenthal, J., Brodie, B.B., 1954. Mechanism of the potentiating action of β-diethylaminoethyl diphenylpropylacetate. J. Pharmacol. Exp. Therapeut. 112, 49–54.

Beland, F.A., 1999. NTP technical report on the toxicity and metabolism studies of chloral hydrate (CAS No. 302-17-0). Administered by gavage to F344/N rats and B6C3F1 mice. Toxic Rep. 59, 1–66 A1-E7.

Bhojani, M.S., Chen, G., Ross, B.D., Beer, D.G., Rehemtulla, A., 2005. Nuclear localized phosphorylated FADD induces cell proliferation and is associated with aggressive lung cancer. Cell Cycle 4, 1478–1481.

Buscà, R., Pouysségur, J., Lenormand, P., 2016. ERK1 and ERK2 Map kinases: specific roles or functional redundancy? Front Cell Dev. Biol. 4, 53. https://doi.org/10.3389/fcell.2016.00053.

Callaway, K., Abramczyk, O., Martin, L., Dalby, K.N., 2007. The anti-apoptotic protein PEA-15 is a tight binding inhibitor of ERK1 and ERK2, which blocks docking interactions at the D-recruitment site. Biochemistry 46, 9187–9198.

Campagna, J.A., Miller, K.W., Forman, S.A., 2003. Mechanisms of actions of inhaled anesthetics. N. Engl. J. Med. 348, 2110–2124.

Catalanotti, F., Reyes, G., Jesenberger, V., Galabova-Kovacs, G., de Matos Simoes, R., Carugo, O., Baccarini, M., 2009. A Mek1-Mek2 heterodimer determines the strength and duration of the Erk signal. Nat. Struct. Mol. Biol. 16, 294–303.

Chou, F.L., Hill, J.M., Hsieh, J.C., Pouyssegur, J., Brunet, A., Glading, A., Uberall, F., Ramos, J.W., Werner, M.H., Ginsberg, M.H., 2003. PEA-15 binding to ERK1/2 MAPKs is required for its modulation of integrin activation. J. Biol. Chem. 278, 52587–52597.

Christopoulos, A., Changeux, J.-P., Catterall, W.A., Fabbro, D., Burris, T.P., Cidlowski, J.A., Olsen, R.W., 2014. International Union of Basic and Clinical Pharmacology. XC. Multisite pharmacology: recommendations for the nomenclature of receptor allosterism and allosteric ligands. Pharmacol. Rev. 66, 918–947.

Coley, A.A., Gao, W.J., 2018. PSD95: a synaptic protein implicated in schizophrenia or autism? Prog. Neuro-Psychopharmacol. Biol. Psychiatry 82, 187–194.

Desarnaud, F., Macone, B.W., Datta, S., 2011. Activation of extracellular signal-regulated kinase signaling in the pedunculopontine tegmental cells is involved in the maintenance of sleep in rats. J. Neurochem. 116, 577–587.

D'Hulst, C., Atack, J.R., Kooy, R.F., 2009. The complexity of the $GABA_A$ receptor shapes unique pharmacological profiles. Drug Discov. Today 14, 866–875.

Dumoulin, M.C., Aton, S.J., Watson, A.J., Renouard, L., Coleman, T., Frank, M.G., 2015. Extracellular signal-regulated kinase (ERK) activity during sleep consolidates cortical plasticity in vivo. Cerebr. Cortex 25, 507–515.

Faci, A., Plaa, G.L., Sharkawi, M., 1998. Chloral hydrate enhances ethanol-induced inhibition of methanol oxidation in mice. Toxicology 131, 1–7.

Ferrer-Alcón, M., García-Sevilla, J.A., Jaquet, P.E., La Harpe, R., Riederer, B.M., Walzer, C., Guimón, J., 2000. Regulation of nonphosphorylated and phosphorylated forms of neurofilament proteins in the prefrontal cortex of human opioid addicts. J. Neurosci. Res. 61, 338–349.

Formstecher, E., Ramos, J.W., Fauquet, M., Calderwood, D.A., Hsieh, J.C., Canton, B., Nguyen, X.T., Barnier, J.V., Camonis, J., Ginsberg, M.H., Chneiweiss, H., 2001. PEA-15 mediates cytoplasmic sequestration of ERK MAP kinase. Dev. Cell 1, 239–250.

Franks, N.P., 2008. General anaesthesia: from molecular targets to neuronal pathways of sleep and arousal. Nat. Rev. Neurosci. 9, 370–386.

García-Fuster, M.J., Miralles, A., García-Sevilla, J.A., 2007. Effects of opiate drugs on Fas-associated protein with death domain (FADD) and effector caspases in the rat brain: regulation by the ERK1/2 MAP kinase pathway. Neuropsychopharmacology 32, 399–411.

García-Fuster, M.J., Ramos-Miguel, A., Miralles, A., García-Sevilla, J.A., 2008. Opioid receptor agonists enhance the phosphorylation state of Fas-associated death domain (FADD) protein in the rat brain: functional interactions with casein kinase Iα, $G\alpha_i$ proteins, and ERK1/2 signaling. Neuropharmacology 55, 886–899.

Garrett, K.M., Gan, J., 1998. Enhancement of γ-aminobutyric $acid_A$ receptor activity by α-chloralose. J. Pharmacol. Exp. Therapeut. 285, 680–686.

Gómez-Angelats, M., Cidlowski, J.A., 2003. Molecular evidence for the nuclear localization of FADD. Cell Death Differ. 10, 791–797.

Harrison, N.L., Kugler, J.L., Jones, M.V., Greenblatt, E.P., Pritchett, D.B., 1993. Positive modulation of human gamma-aminobutyric acid type A and glycine receptors by the inhalation anesthetic isoflurane. Mol. Pharmacol. 44, 628–632.

Hentschke, H., Raz, A., Krause, B.M., Murphy, C.A., Banks, M.I., 2017. Disruption of cortical network activity by the general anaesthetic isoflurane. Br. J. Anaesth. 119, 685–696.

Imtiyaz, H.Z., Zhou, X., Zhang, H., Chen, D., Hu, T., Zhang, J., 2009. The death domain of FADD is essential for embryogenesis, lymphocyte development, and proliferation. J. Biol. Chem. 284, 9917–9926.

Jeon, S.J., Park, H.J., Gao, Q., Pena, I.J., Park, S.J., Lee, H.E., Woo, H., Kim, H.J., Cheong, J.H., Hong, E., Ryu, J.H., 2015. Ursolic acid enhances pentobarbital-induced sleeping behaviors via GABAergic neurotransmission in mice. Eur. J. Pharmacol. 762, 443–448.

Jia, F., Yue, M., Chandra, D., Homanics, G.E., Goldstein, P.A., Harrison, N.L., 2008. Isoflurane is a potent modulator of extrasynaptic $GABA_A$ receptors in the thalamus. J. Pharmacol. Exp. Therapeut. 324, 1127–1135.

Kalluri, H.S.G., Ticku, M.K., 2002. Role of $GABA_A$ receptors in the ethanol-mediated inhibition of extracellular signal-regulated kinase. Eur. J. Pharmacol. 451, 51–54.

Knodell, R.G., Spector, M.H., Brooks, D.A., Keller, F.X., Kyner, W.T., 1980. Alterations in pentobarbital pharmacokinetics in response to parenteral and enteral alimentation in the rat. Gastroenterology 79, 1211–1216.

Krueger, J., Chou, F.-L., Glading, A., Schaefer, E., Ginsberg, M.H., 2005. Phosphorylation of phosphoprotein enriched in astrocytes (PEA-15) regulates extracellular signal-regulated kinase-dependent transcription and cell proliferation. Mol. Biol. Cell 16, 3552–3561.

Kumar, S., Porcu, P., Werner, D.F., Matthews, D.B., Diaz-Granados, J.L., Helfand, R.S., Morrow, A.L., 2009. The role of $GABA_A$ receptors in the acute and chronic effects of ethanol: a decade of progress. Psychopharmacology (Berlin) 205, 529–564.

Leikas, J.V., Kohtala, S., Theilmann, W., Jalkanen, A.J., Forsberg, M.M., Rantamäki, T., 2017. Brief isoflurane anesthesia regulates striatal AKT-GSK3β signaling and ameliorates motor deficits in a rat model of early-stage Parkinson's disease. J. Neurochem. 142, 456–463.

Mace, P.D., Wallez, Y., Egger, M.F., Dobaczewska, M.K., Robinson, H., Pasquale, E.B., Riedl, S.J., 2013. Structure of ERK2 bound to PEA-15 reveals a mechanism for rapid release of activated MAPK. Nat. Commun. 4, 1681.

Mihic, S.J., Harris, R.A., 2011. Hypnotics and sedatives. Chapter 17 In: Brunton, L.L. (Ed.), Goodman & Gilman's the Pharmacological Basis of Therapeutics, twelfth ed. McGraw-Hill Medical, New York, pp. 457–480.

Moranta, D., Esteban, S., García-Sevilla, J.A., 2007. Acute, chronic and withdrawal effects of the cannabinoid receptor agonist WIN55212-2 on the sequential activation of MAPK/Raf-MEK-ERK signaling in the rat cerebral frontal cortex: short-term

regulation by intrinsic and extrinsic pathways. J. Neurosci. Res. 85, 656–667.
Olsen, R.W., 2015. Allosteric ligands and their binding sites define γ-aminobutyric acid (GABA) type A receptor subtypes. Adv. Pharmacol. 73, 167–202.
Patel, P.M., Patel, H.H., Roth, D.M., 2011. General anesthetics and therapeutic gases. Chapter 19 In: Brunton, L.L. (Ed.), Goodman & Gilman's the Pharmacological Basis of Therapeutics, twelfth ed. McGraw-Hill Medical, New York, pp. 527–564.
Pearson, G., Robinson, F., Beers Gibson, T., Xu, B.E., Karandikar, M., Berman, K., Cobb, M.H., 2001. Mitogen-activated protein (MAP) kinase pathways: regulation and physiological functions. Endocr. Rev. 22, 153–183.
Ramos-Miguel, A., García-Sevilla, J.A., 2012. Crosstalk between cdk5 and MEK-ERK signalling upon opioid receptor stimulation leads to upregulation of activator p25 and MEK1 inhibition in rat brain. Neuroscience 215, 17–30.
Ramos-Miguel, A., Esteban, S., García-Sevilla, J.A., 2010. The time course of unconditioned morphine-induced psychomotor sensitization mirrors the phosphorylation of FADD and MEK/ERK in rat striatum: role of PEA-15 as a FADD-ERK binding partner in striatal plasticity. Eur. Neuropsychopharmacol 20, 49–64.
Ramos-Miguel, A., Miralles, A., García-Sevilla, J.A., 2011. Correlation of rat cortical Fas-associated death domain (FADD) protein phosphorylation with the severity of spontaneous morphine abstinence syndrome: role of α_2-adrenoceptors and extracellular signal-regulated kinases. J. Psychopharmacol. 25, 1691–1702.
Ramos-Miguel, A., García-Fuster, M.J., Callado, L.F., La Harpe, R., Meana, J.J., García-Sevilla, J.A., 2009. Phosphorylation of FADD (Fas-associated death domain protein) at serine 194 is increased in the prefrontal cortex of opiate abusers: relation to mitogen activated protein kinase, phosphoprotein enriched in astrocytes of 15 kDa, and Akt signaling pathways involved in neuroplasticity. Neuroscience 161, 23–38.
Ramos-Miguel, A., Álvaro-Bartolomé, M., García-Fuster, M.J., García-Sevilla, J.A., 2012. Role of multifunctional FADD (Fas-Associated Death Domain) adaptor in drug addiction. Chapter 7 In: Belin, David (Ed.), Addictions–from Pathophysiology to Treatment. In Tech Open, Rijeka, Croatia, 978-953-51-0783-5, pp. 201–226.
Rao, S.G., Williams, G.V., Goldman-Rakic, P.S., 2000. Destruction and creation of spatial tuning by disinhibition: $GABA_A$ blockade of prefrontal cortical neurons engaged by working memory. J. Neurosci. 20, 485–494.
Robinson, F.L., Whitehurst, A.W., Raman, M., Cobb, M.H., 2002. Identification of novel point mutations in ERK2 that selectively disrupt binding to MEK1. J. Biol. Chem. 277, 14844–14852.
Roskoski Jr., R., 2012a. MEK1/2 dual-specificity protein kinases: structure and regulation. Biochem. Biophys. Res. Commun. 417, 5–10.
Roskoski Jr., R., 2012b. ERK1/2 MAP kinases: structure and regulation. Pharmacol. Res. 66, 105–143.
Saari, T.I., Uusi-Oukari, M., Ahonen, J., Olkkola, K.T., 2011. Enhancement of GABAergic activity: neuropharmacological effects of benzodiazepines and therapeutic use in anesthesiology. Pharmacol. Rev. 63, 243–267.
Salles, A., Romano, A., Freudenthal, R., 2014. Synaptic NF-kappa B pathway in neuronal plasticity and memory. J. Physiol. Paris 108, 256–262.
Salort, G., Álvaro-Bartolomé, M., García-Sevilla, J.A., 2019. Ketamine-induced hypnosis and neuroplasticity in mice is associated with disrupted p-MEK/p-ERK sequential activation and sustained upregulation of survival p-FADD in brain cortex: involvement of $GABA_A$ receptor. Prog. Neuro-Psychopharmacol. Biol. Psychiatry 88, 121–131.
Schwartz, J.R.L., Roth, T., 2008. Neurophysiology of sleep and wakefulness: basic science and clinical implications. Curr. Neuropharmacol. 6, 367–378.
Seibt, J., Aton, S.J., Jha, S.K., Coleman, T., Dumoulin, M.C., Frank, M.G., 2008. The non-benzodiazepine hypnotic zolpidem impairs sleep-dependent cortical plasticity. Sleep 31, 1381–1391.
Sharko, A.C., Hodge, C.W., 2008. Differential modulation of ethanol-induced sedation and hypnosis by metabotropic glutamate receptor antagonists in C57BL/6J mice. Alcohol Clin. Exp. Res. 32, 67–76.
Shen, C.P., Tsimberg, Y., Salvadore, C., Meller, E., 2004. Activation of Erk and JNK MAPK pathways by acute swim stress in rat brain regions. BMC Neurosci. 5, 36.
Shroads, A.L., Coats, B.S., Langaee, T., Shuster, J.J., Stacpoole, P.W., 2015. Chloral hydrate, through biotransformation to dichloroacetate, inhibits maleylacetoacetate isomerase and tyrosine catabolism in humans. Drug Metab. Pers. Ther. 30, 49–55.
Steinbach, J.H., Akk, G., 2001. Modulation of $GABA_A$ receptor channel gating by pentobarbital. J. Physiol. 537 (3), 715–733.
Suzdak, P.D., Glowa, J.R., Crawley, J.N., Schwartz, R.D., Skolnick, P., Paul, S.M., 1986. A selective imidazobenzodiazepine antagonist of ethanol in the rat. Science 234, 1243–1247.
Sweatt, J.D., 2001. The neuronal MAP kinase cascade: a biochemical signal integration system subserving synaptic plasticity and memory. J. Neurochem. 76, 1–10.
Takamura, H., Ichisaka, S., Watanabe, K., Toigawa, M., Hata, Y., 2008. Effects of anesthesia on immunohistochemical detection of phosphorylated extracellular signal-regulated kinase in cerebral cortex. J. Neurosci. Methods 170, 300–304.
Tourneur, L., Chiocchia, G., 2010. FADD: a regulator of life and death. Trends Immunol. 31, 260–269.
Vahle-Hinz, C., Detsch, O., Siemers, M., Kochs, E., Bromm, B., 2001. Local $GABA_A$ receptor blockade reverses isoflurane's suppressive effects on thalamic neurons in vivo. Anesth. Analg. 92, 1578–1584.
Whittington, R.A., Bretteville, A., Virág, L., Emala, C.W., Maurin, T.O., Marcouiller, F., Julien, C., Petry, F.R., El-Khoury, N.B., Morin, F., Charron, J., Planel, E., 2013. Anesthesia-induced hypothermia mediates decreased ARC gene and protein expression through ERK/MAPK inactivation. Sci. Rep. 3, 1388.
Xie, J., Li, Y., Huang, Y., Qiu, P., Shu, M., Zhu, W., Ou, Y., Yan, G., 2009. Anesthetic pentobarbital inhibits proliferation and migration of malignant glioma cells. Cancer Lett. 282, 35–42.
Yang, G., Lai, C.S., Cichon, J., Ma, L., Li, W., Gan, W.B., 2014. Sleep promotes branch-specific formation of dendritic spines after learning. Science 344, 1173–1178.
Yoon, S., Seger, R., 2006. The extracellular signal-regulated kinase: multiple substrates regulate diverse cellular functions. Growth Factors 24, 21–44.
Zanger, U.M., Schwab, M., 2013. Cytochrome P450 enzymes in drug metabolism: regulation of gene expression, enzyme activities, and impact of genetic variation. Pharmacol. Ther. 138, 103–141.
Zeller, A., Arras, M., Jurd, R., Rudolph, U., 2007. Identification of a molecular target mediating the general anesthetic actions of pentobarbital. Mol. Pharmacol. 71, 852–859.
Zhang, J., Zhang, D., Hua, Z., 2004. FADD and its phosphorylation. IUBMB Life 56, 395–401.